Cellular Microbiology (2015) **17**(3), 389–407
doi:10.1111/cmi.12374
First published online 22 November 2014

Compositional and immunobiological analyses of extracellular vesicles released by *Candida albicans*

Gabriele Vargas,[1] Juliana D. B. Rocha,[2] Debora Leite Oliveira,[1] Priscila Costa Albuquerque,[1] Susana Frases,[2] Suelen S. Santos,[3] Joshua Daniel Nosanchuk,[4,5] Andre Marco Oliveira Gomes,[6] Lia C. A. S. Medeiros,[2] Kildare Miranda,[2] Tiago J. P. Sobreira,[7] Ernesto S. Nakayasu,[8] Emma A. Arigi,[9] Arturo Casadevall,[4] Allan J. Guimaraes,[10] Marcio L. Rodrigues,[1,11] Celio Geraldo Freire-de-Lima,[2] Igor C. Almeida[9] and Leonardo Nimrichter[1]*

[1]*Instituto de Microbiologia Paulo de Góes, Universidade Federal do Rio de Janeiro (UFRJ), Rio de Janeiro, RJ, Brazil.*
[2]*Instituto de Biofísica Carlos Chagas Filho, Universidade Federal do Rio de Janeiro (UFRJ), Rio de Janeiro, RJ, Brazil.*
[3]*Faculdade de Ciências Farmacêuticas, Universidade de São Paulo, São Paulo, SP, Brazil.*
[4]*Programa de Biologia Estrutural, Instituto de Bioquímica Médica Leopoldo DeMeis, Universidade Federal do Rio de Janeiro (UFRJ), Rio de Janeiro, Brazil.*
[5]*Instituto Nacional de Ciência e Tecnologia de Biologia Estrutural e Bioimagem, Universidade Federal do Rio de Janeiro (UFRJ), Rio de Janeiro, Brazil.*
[6]*Departments of Medicine and Microbiology & Immunology, Albert Einstein College of Medicine, New York, USA.*
[7]*National Laboratory for Biosciences (LNBio), National Center for Research in Energy and Materials, Campinas, SP 13083-970, Brazil.*
[8]*Bindley Bioscience Center, Purdue University, West Lafayette, IN 47907, USA.*
[9]*The Border Biomedical Research Center, Department of Biological Sciences, University of Texas at El Paso, El Paso, TX 79968, USA.*
[10]*Departamento de Microbiologia e Parasitologia, Universidade Federal Fluminense, Rio de Janeiro, RJ, Brazil.*
[11]*Centro de Desenvolvimento Tecnológico em Saúde (CDTS) da Fundação Oswaldo Cruz (Fiocruz), Rio de Janeiro, Brazil.*

Received 25 September, 2013; revised 8 September, 2014; accepted 22 September, 2014. *For correspondence. E-mail nimrichter@micro.ufrj.br; Tel. (+55) 21 2562 6743 (x141); Fax (+55) 21 2560 8344.

Summary

The release of extracellular vesicles (EV) by fungal organisms is considered an alternative transport mechanism to trans-cell wall passage of macromolecules. Previous studies have revealed the presence of EV in culture supernatants from fungal pathogens, such as *Cryptococcus neoformans*, *Histoplasma capsulatum*, *Paracoccidioides brasiliensis*, *Sporothrix schenckii*, *Malassezia sympodialis* and *Candida albicans*. Here we investigated the size, composition, kinetics of internalization by bone marrow-derived murine macrophages (MO) and dendritic cells (DC), and the immunomodulatory activity of *C. albicans* EV. We also evaluated the impact of EV on fungal virulence using the *Galleria mellonella* larvae model. By transmission electron microscopy and dynamic light scattering, we identified two populations ranging from 50 to 100 nm and 350 to 850 nm. Two predominant seroreactive proteins (27 kDa and 37 kDa) and a group of polydispersed mannoproteins were observed in EV by immunoblotting analysis. Proteomic analysis of *C. albicans* EV revealed proteins related to pathogenesis, cell organization, carbohydrate and lipid metabolism, response to stress, and several other functions. The major lipids detected by thin-layer chromatography were ergosterol, lanosterol and glucosylceramide. Short exposure of MO to EV resulted in internalization of these vesicles and production of nitric oxide, interleukin (IL)-12, transforming growth factor-beta (TGF-β) and IL-10. Similarly, EV-treated DC produced IL-12p40, IL-10 and tumour necrosis factor-alpha. In addition, EV treatment induced the up-regulation of CD86 and major histocompatibility complex class-II (MHC-II). Inoculation of *G. mellonella* larvae with EV followed by challenge with *C. albicans* reduced the number of recovered viable yeasts in comparison with infected larvae control. Taken together, our results demonstrate that *C. albicans* EV were immunologically active and could potentially interfere with the host responses in the setting of invasive candidiasis.

Introduction

Candida species are the most common fungal pathogens to cause invasive disease in humans (Hazen, 1995; Pfaller and Diekema, 2007). Although the incidence of non-*albicans* species of *Candida* has increased in the last decades, *Candida albicans* remains the most prevalent species isolated from patients with invasive candidiasis (Nucci *et al*., 2010; Kim and Sudbery, 2011). In healthy individuals, *C. albicans* growth is controlled by different host elements, including epithelial barriers, the immune system and microbial flora (Cheng *et al*., 2012; Gow and Hube, 2012a). However, when immunological breakdowns occur, *C. albicans* may proliferate resulting in disease states ranging from superficial to disseminated, lethal infections (Cheng *et al*., 2012). The major risk factors to develop invasive candidiasis include HIV infection, neutropoenia, use of intravenous catheters, exposure to systemic antibacterial drugs and prolonged periods in intensive care units (Concia *et al*., 2009; Kim and Sudbery, 2011). The most commonly prescribed drug to combat *C. albicans* is fluconazole (Azie *et al*., 2012). Amphotericin B formulations, echinocandins and voriconazole are often used for non-*albicans* infections, but are also alternatives to combat *C. albicans* (Pappas *et al*., 2004). Despite the current arsenal for treatment, *Candida* infections are nevertheless associated with significant morbidity and mortality rates (Pfaller and Diekema, 2007; Arendrup, 2010). Several studies suggest that adjuvant immunotherapy is a potential alternative for the treatment of candidiasis (van de Veerdonk *et al*., 2012), or for use in combination with antifungal drugs.

The interplay between *C. albicans* and the innate immune system influences the conversion between saprophytic and parasitic stages (Cheng *et al*., 2012). Inflammatory cytokines such as tumour necrosis factor-alpha (TNF-α), interleukin (IL)-1β, IL-6, and interferon-γ are associated with the control of candidiasis (Romani, 2000), whereas IL-10 and IL-4 can facilitate an immunosuppressive response favouring *C. albicans* dissemination (Romani, 2000). Pattern recognition receptors (PRRs) at the surface of phagocytic cells distinguish among the polysaccharides and glycoconjugates composing the cell wall network (Heinsbroek *et al*., 2005; Jouault *et al*., 2009; Netea and Marodi, 2010). However, the immune response to candidiasis and other infections is not exclusively dependent on pathogen–host cell engagement. Secreted components from pathogens frequently engage host PRRs, which results in modulation of the host immune response profile.

In fungal infections, secretory mechanisms are key events for disease establishment (Batanghari *et al*., 1998; Naglik *et al*., 2003b; Kmetzsch *et al*., 2011). For example, virulence of *C. albicans* is associated with constitutive secretion of proteases (Braga-Silva and Santos, 2011) and lipase (Gacser *et al*., 2007). Recently, Sorgo and colleagues characterized 44 proteins in the secretome of *C. albicans*, including hydrolases such as secreted aspartyl proteases (SAPs), chitinase, β-1,3 glucanase, hexosaminidase and superoxide dismutase (Sorgo *et al*., 2010). The adhesins Als3 and Als4 were also detected in *C. albicans* supernatants. The identification of these virulence-associated molecules is consistent with the fact that mutants with defective secretion pathways are less virulent in murine models of candidiasis and these disruptants also have defective branching and biofilm formation (Newport *et al*., 2003; Thomas *et al*., 2009).

Recent findings demonstrate that fungal organisms release many molecular components to the extracellular space in extracellular vesicles (EV) (Rodrigues *et al*., 2007; 2008; Albuquerque *et al*., 2008a; Gehrmann *et al*., 2011; Vallejo *et al*., 2011). Proteins, polysaccharides, lipids and pigments have been characterized in fungal EV isolated from culture supernatants of *Cryptococcus neoformans*, *Paracoccidioides brasiliensis*, *Saccharomyces cerevisiae* and *Histoplasma capsulatum* (Rodrigues *et al*., 2007; 2008; Albuquerque *et al*., 2008a; Vallejo *et al*., 2011). In *C. neoformans*, EV are associated with polysaccharide (GXM) export and capsular growth (Rodrigues *et al*., 2007). Cryptococcal EV modulate macrophage (MO) cytokines, stimulate nitric oxide (NO) production and increase the fungicidal activity of these cells (Oliveira *et al*., 2010a). Gehrmann and colleagues have shown that EV from *Malassezia sympodialis* elicit enhanced IL-4 production by CD14 and CD34-depleted peripheral blood mononuclear cells from patients with atopic eczema, when compared with healthy individuals (Gehrmann *et al*., 2011). TNF-α was induced by *M. sympodialis* EV in both groups.

In *C. albicans*, the occurrence of EV was first suggested by Anderson *et al*. (1990). These authors demonstrated vesicle-like compartments in cell wall pimples from opaque cultures of *C. albicans* yeast cells. *C. albicans* EV were first isolated and observed by transmission electron microscopy (TEM) by Albuquerque *et al*. (2008a), who demonstrated the presence of bilayered compartments similar to those initially described for *C. neoformans* and *H. capsulatum* (Rodrigues *et al*., 2007; Albuquerque *et al*., 2008a). Compositional and functional aspects of *C. albicans* EV, however, have remained unknown. Here, we characterized dimensions, protein composition and immunomodulatory activity of *C. albicans* EV. In addition, we demonstrated that pretreatment with EV from *C. albicans* reduced yeast viability in a *Galleria mellonella* model of infection. Our results reveal a complex array of protein and lipid components in *C. albicans* EV that could

modulate the activity of MOs and dendritic cells (DCs) as well as interfere with disease pathogenesis in *G. mellonella*.

Results

Morphological characterization of C. albicans *EV*

TEM analysis of vesicular preparations showed round bilayered compartments with variable dimensions and electron densities (Fig. 1A). Based on TEM images, *C. albicans* EV appeared to be free of contaminant dead cells and organelles. Using a cryoultramicrotomy-based approach previously optimized for *C. neoformans* (Oliveira *et al*., 2009), high-resolution images of *C. albicans* cells were generated, as denoted by the presence of well-preserved membranous structures (Fig. 1B). Bilayered, membranous vesicles were observed at the periplasmic space of *C. albicans* yeast cells. Cell wall vesicles, however, were not clearly observed, which is likely due to the high electron density of this fungal compartment. As TEM uses sequential sections, dimensional determination of EV is imprecise. We therefore analysed EV dimensions by dynamic light scattering, a method extensively used to measure liposomes and recently used to measure fungal vesicles (Eisenman *et al*., 2009; Oliveira *et al*., 2010b). Two different strains of *C. albicans* (11 and ATCC 90028) were used to evaluate the dimensional heterogeneity of these compartments (Fig. 1C). Both strains produced vesicles ranging between 50 and 100 nm in diameter. However, the ATCC strain displayed a population of larger vesicles raging from 450 to 850 nm, whereas the strain 11 displayed a second set of vesicles varying from 350 to 450 nm. These data confirmed that fungal EV are considerably heterogeneous even among the same species.

C. albicans *EV show a complex composition*

Previous studies reported that fungal EV carry diverse proteins, lipids, polysaccharides and pigments (Rodrigues *et al*., 2008; Oliveira *et al*., 2010a,b; Vallejo *et al*., 2011; 2012a,b). To analyse the lipid content, *C. albicans* EV were extracted with organic solvents. The resulting molecules were partitioned and resolved by high-performance thin-layer chromatography (HPTLC). The lipids found were ergosterol and the neutral glycosphingolipid (GSL) glucosylceramide (GlcCer) (Fig. 2A), recently described as a key virulence regulator of *C. albicans* and *C. neoformans* (Rittershaus *et al*., 2006; Noble *et al*., 2010). Both structures have been reported previously as components of EV in *C. neoformans* (Rodrigues *et al*., 2007), thus supporting our data. Supernatants from heat-killed yeasts were also fractionated for vesicle isolation to confirm that EV detection was not an artefact resulting from the release of internal organelles from dead cells and/or cell debris. Ultracentrifugation pellets gave negative results for the presence of lipids (data not shown), confirming that EV are only released by live yeast cells. Protein components of *C. albicans* EV were initially analysed by silver staining after sodium dodecyl sulfate polyacrylamide gel electrophoresis

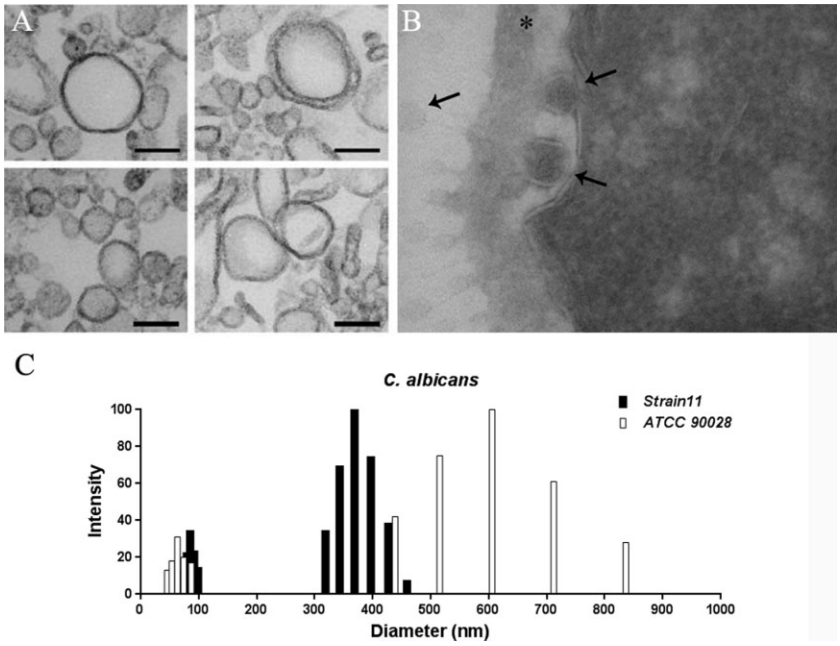

Fig. 1. Morphological and dimensional aspects of *Candida albicans* EV.
A. TEM of isolated EV (strain ATCC 90028). Scale bar, 100 nm.
B. TEM images of a *C. albicans* yeast cell showing the presence of EV at both periplasmic and extracellular spaces (strain 11). Asterisk indicates cell wall. Arrows indicate vesicles. Scale bar 200 nm.
C. Distribution of EV dimensions. Vesicles were isolated from strains 11 and ATCC 90028 and subjected to dynamic light scattering analysis.

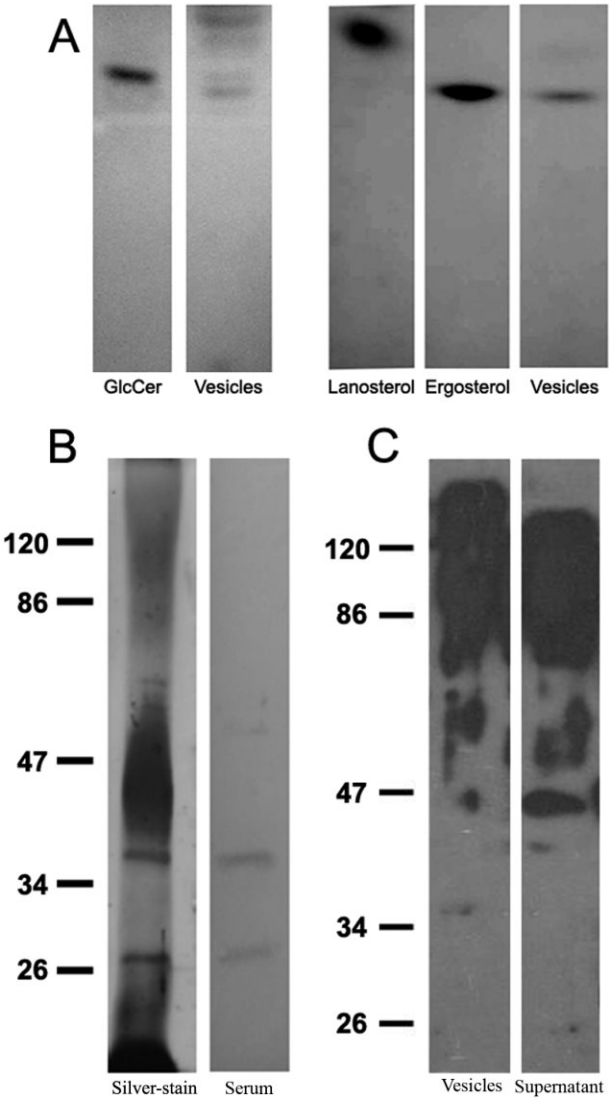

Fig. 2. EV produced by *Candida albicans* contain neutral lipids and protein components.
A. Total lipids were extracted from strain 11 with organic solvents and partitioned in biphasic water-organic mixtures. Lipid components with migration rates corresponding to GlcCer and sterol were detected by thin-layer chromatography.
B. Protein content associated to vesicles was visualized by silver staining (SS, left lane). Two major vesicle proteins were recognized by sera from infected mice (Sm, right lane).
C. The presence of mannosylated proteins was detected using ConA, which recognizes α-mannosyl-linked residues. Lan, lanosterol; Erg, ergosterol; SS, silver stain; Sm, serum and S, supernatant. Relative molecular mass markers (KDa) are indicated on the left of B and C.

(SDS-PAGE) (Fig. 2B). These proteins were blotted onto nitrocellulose membranes and probed with sera obtained from mice infected with *C. albicans*. As previously demonstrated for *H. capsulatum* and *C. neoformans* (Albuquerque *et al.*, 2008a; Oliveira *et al.*, 2010a), seroreactive proteins were found in *C. albicans* vesicles. Two prominent bands of approximately 27 kDa and 37 kDa that reacted with serum from *C. albicans*-infected mice were detected (Fig. 2B). As mannoproteins are constitutively released by *C. albicans* (Calderone and Wadsworth, 1987; Torosantucci *et al.*, 1991; Lopez-Ribot *et al.*, 1995), we asked whether secretion of these glycoproteins was also linked to EV production. Figure 2C shows a representative result of immunoblots of protein extracts from *C. albicans* EV or culture supernatants after incubation with horseradish peroxidase (HRP)-labelled concanavalin A (ConA). The patterns of lectin staining were similar in both samples, consistent with highly polydispersed mannoproteins with relatively high molecular masses (80–130 kDa). Bands were also visualized between the relative molecular mass range of 44 and 80 kDa.

Considering that the protein profile of EV produced by *C. albicans* is unknown, we analysed these membranous compartments by proteomics. EV from strains 11 and ATCC 90028 were investigated, allowing for the identification of 57 protein groups (Table 1 and Supporting Information Table S1A–D). As observed in Supporting Information Table S1A, 35 protein groups (i.e. 10–12, 18, 20–23, 25–28, 30–37, 39, 43–51 and 53–57) were identified in strain 11, but not ATCC 90028, 15 protein groups (i.e. 1–9, 13–15, 17, 19, and 24) were identified in both strains and only seven protein groups (16, 29, 38, 40–42, and 52) were identified in strain ATCC 90028, but not in strain 11. These differentially identified protein groups are highlighted in the Supporting Information Table S1A and indicated in Table 1. However, as our proteomic analysis was not quantitative, that is, carried out with at least three to five technical replicates of each biological sample, and not performed with at least two biological replicates, we would rather not speculate about the differential expression of the distinct protein groups in the two strains analysed.

The proposed molecular and biological functions of these proteins with references are shown in Supporting Information Table S2. Using the UniProt database, the proteins were classified according to their putative functions in the fungal cells (Fig. 3), including (i) pathogenesis (22), (ii) cell organization and biogenesis (20), (iii) carbohydrate and lipid metabolism (18), (iv) stimulation of host defences (12), (v) response to stress (4), (vi) protein metabolism (3) and (vii) unknown functions (12). This type of analysis allowed the distribution of the same protein in more than one functional class. We also classified proteins according to their cellular distribution (Fig. 3B). Most vesicular proteins were associated with cell wall (29), cytoplasm (21), extracellular environment (17) and plasma membrane (16). Thirteen proteins had undetermined cellular location and only two molecules were identified as nuclear proteins. The presence of proteins

Table 1. List of protein groups identified by proteomic analysis of extracellular vesicles from *C. albicans* strains 11 and ATCC 90028.

Protein group number	Protein name	Accession number	Protein group identification[a]	
			Strain 11	Strain ATCC 90028
1	Enolase 1	P30575	+	+
2	Glyceraldehyde-3-phosphate dehydrogenase	Q5ADM7	+	+
3	Cell wall glucanase (MP65)	Q59XS9	+	+
4	Putative uncharacterized protein UTH1	Q5AKU5	+	+
5	Pyruvate decarboxylase	P83779	+	+
6	Cell wall glucanase (SCW11)	Q5AKC7	+	+
7	Putative uncharacterized protein TOS1	Q5AJN2	+	+
8	Glycosyl hydrolase	Q5AMT2	+	+
9	Cell surface flocculin	Q5ALT5	+	+
10	Phospholipase B3	Q5AMD3	+	–
11	Fructose-bisphosphate aldolase	Q9URB4	+	–
12	SUN family beta-glucosidase-like protein	Q59NP5	+	–
13	Chitinase 2	P40953	+	+
14	Chitinase 3	P40954	+	+
15	pH-responsive protein 2	O13318	+	+
16	Putative uncharacterized protein	Q5AF30	–	+
17	Putative uncharacterized protein	P82612	+	+
18	Phosphoglycerate kinase	P46273	+	–
19	Putative uncharacterized protein UTR2	Q5AJC0	+	+
20	Heat shock protein SSA1 HSP70	P41797	+	–
21	pH-regulated antigen PRA1/58 kDa fibrinogen-binding mannoprotein	P87020	+	–
22	Transaldolase	Q5A017	+	–
23	Potential alkyl hydroperoxide reductase	Q5AF44	+	–
24	Putative NADPH-dependent methylglyoxal reductase GRP2	P83775	+	+
25	Triosephosphate isomerase	Q9P940	+	–
26	Candidapepsin-2	C4YMJ3	+	–
27	Putative uncharacterized protein TKT1	Q5A750	+	–
28	Potential alpha-1,6-mannanase	Q59QH2	+	–
29	Potential alpha-1,6-mannanase	Q59XY6	–	+
30	Putative uncharacterized protein HSP12	Q5AGU9	+	–
31	Thiamine thiazole synthase	Q5ANB7	+	–
32	Elongation factor 2	Q5A0M4	+	–
33	Peroxiredoxin TSA1	Q9Y7F0	+	–
34	Putative uncharacterized protein	Q5AEL7	+	–
35	Secretory aspartyl proteinase SAP9p	Q59SU1	+	–
36	Candidapepsin-2	P0DJ06	+	–
37	Alcohol dehydrogenase 2	O94038	+	–
38	Potential glycosyl hydrolase/MP65	Q59XX2	–	+
39	Protein YOP1	C4YKB0	+	–
40	Aminopeptidase 2	Q59KZ1	–	+
41	Putative uncharacterized protein	C4YEV7	–	+
42	Agglutinin-like ALS4 protein	Q59L09	–	+
43	Candidapepsin-1	P0CY27	+	–
44	Ras-like protein 1	Q59XU5	+	–
45	Putative uncharacterized protein SSB1	Q5A397	+	–
46	Putative uncharacterized protein	C4YDW6	+	–
47	Agglutinin-like ALS4 protein	Q59L09	+	–
48	Likely cytosolic ribosomal protein L5	Q5AGZ7	+	–
49	Potential protein disulfide isomerase	Q5A9W8	+	–
50	Protein OS-9 homolog	Q5ACR4	+	–
51	Elongation factor 1-alpha 1	P0CY35	+	–
52	Potential cell wall protein	Q59Q33	–	+
53	Translationally controlled tumour protein homolog	Q5A860	+	–
54	Nucleoside diphosphate kinase	Q5AG68	+	–
55	Putative uncharacterized protein / PGA45	Q5AA33	+	–
56	Putative uncharacterized protein ENG1	Q5AHY6	+	–
57	6-Phosphogluconate dehydrogenase, decarboxylating	Q5AKV3	+	–

a. See Supporting Information Table S1A.

associated with pathogenesis and stimulation of host responses in the vesicle proteome led us to investigate whether vesicles from *C. albicans* interact with and stimulate MO and DC.

C. albicans *EV are internalized by MOs and DCs*

To address whether host cells recognize *C. albicans* EV, the isolated membrane compartments were stained with

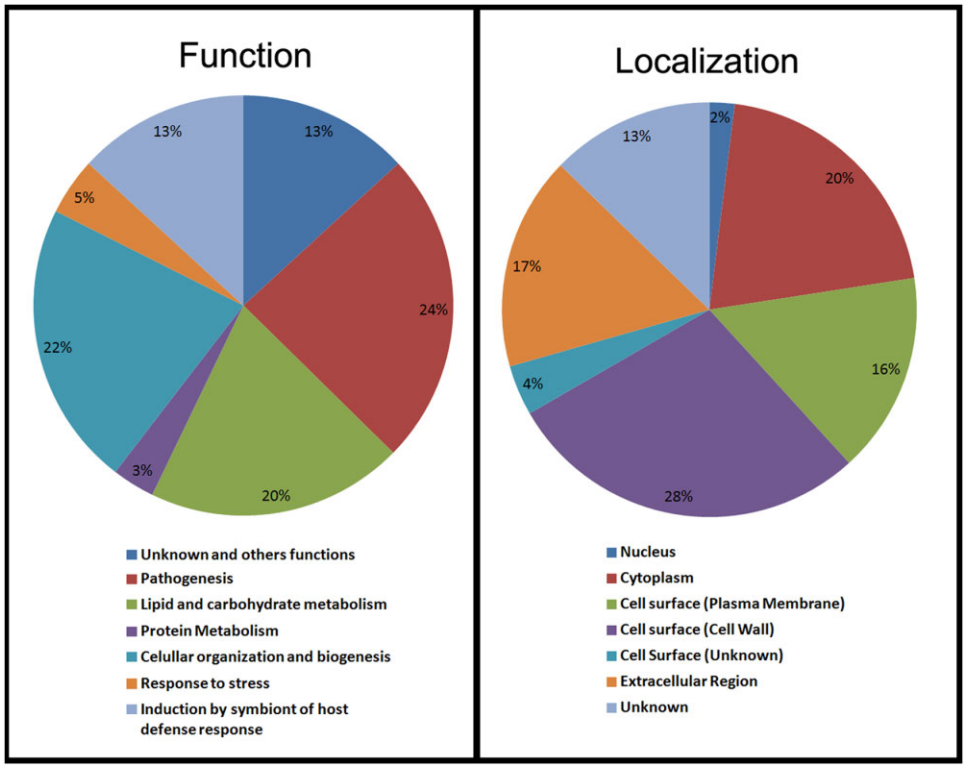

Fig. 3. Classification of EV proteins. Vesicular proteins from strains 11 and ATCC 90028 were identified by mass spectrometry and classified according to their functions and cellular localization.

the red-fluorescent lipophilic stain 1,1′-dioctadecyl-3,3,3,3′-tetramethyl-indocarbocyanine perchlorate ($DiIC_{18}$). This compound intercalates between membrane lipids and has been used to label EV produced by *C. neoformans* (Oliveira *et al.*, 2010a). We evaluated binding and internalization of *C. albicans* EV by MOs and DC using laser scanning confocal fluorescence microscopy or wide field fluorescence microscopy followed or not by deconvolved analysis. After 5 min of exposure of the MOs to the vesicles, the red fluorescence (EV-derived) was associated with the plasma membrane (Fig. 4). A clear co-localization was observed between $DiIC_{18}$-labelled vesicles and the MO plasma membrane lipid GM1, suggesting the involvement of lipid rafts in EV–host cell association (Fig. 4, merged images). We then monitored the fate of EV in MOs for 15 min, 1 h and 16 h. Vesicles were completely internalized by MOs after 15 min incubation and were found randomly dispersed at cytoplasm (Fig. 4). Notably, after 1 h, we visualized a partial compartmentalization of internalized vesicles within the MOs (Fig. 4). The kinetic of vesicle internalization by DC was similar to that observed for the MOs (Fig. 4).

NO and cytokine production is modulated by EV in both MOs and DCs. Vesicles produced by bacteria are potent activators of host cells (Kuehn and Kesty, 2005). On the other hand, the immunomodulatory activity of fungal EV is poorly understood. In this context, we investigated the regulatory effect of EV produced by *C. albicans* in murine MO and DC. Overnight incubation of RAW 264.7 phagocytes or bone marrow (BM)-derived MO with EV from *C. albicans* induced NO production in a dose-dependent fashion (Fig. 5A). Particularly, BM-derived MOs were more efficient in producing NO. A plateau was reached when a vesicle preparation with sterol concentration corresponding to ≥ 4 μM was added to the MO monolayer. We also examined the cytokine profile in supernatants of MOs or DC treated with vesicles from *C. albicans*. EV-treated RAW 264.7 cells produced relatively high amounts of IL-12 and showed a minor increase of transforming growth factor-beta (TGF-β) and IL-10 production, compared with controls (Fig. 5B). When BM-derived MO were incubated with EV, higher levels of IL-12p40, IL-10 and TNF-α were detected with a slight increase of TGF-β (Fig. 5C). These results suggested that the response of primary cells or MO cultures to EV from *C. albicans* is not identical. Production of cytokine was also stimulated after vesicle treatment of DC. Synthesis of IL-12, IL-10, TGF-β and TNF-α was significantly increased in comparison with non-stimulated DC (Fig. 5D). Together, these data suggest that EV from

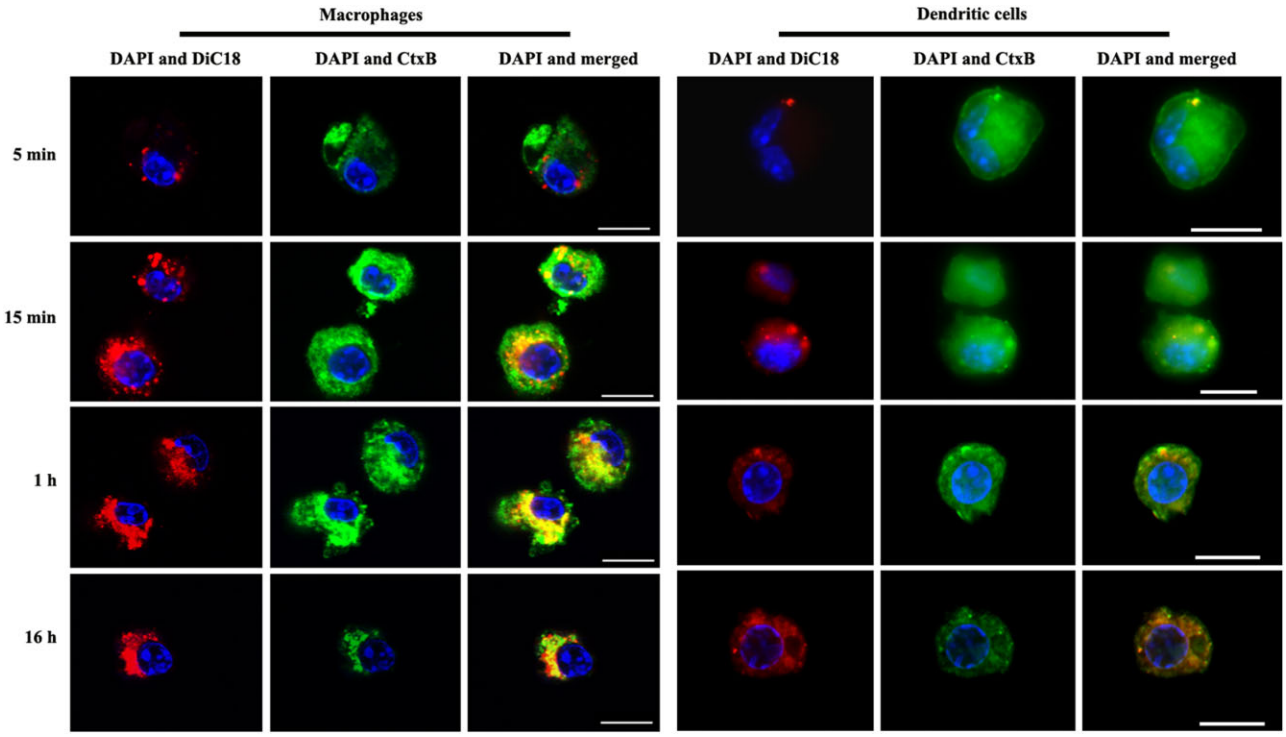

Fig. 4. Internalization of vesicle components by BM-derived MOs and DCs. DiIC18 (red)-stained vesicles (strain 11) were incubated with MOs or DCs at different time points. The plasma membrane ganglioside GM1 (a lipid raft marker) and nuclei were stained with cholera FITC-toxin subunit B (CtxB, green) and DAPI (blue) respectively. Co-localization of GM1 and $DiIC_{18}$-vesicles is evident in merged images. MOs were observed by confocal fluorescence microscopy as described under Experimental Procedures. $z = 0.8$ μm. Bars: 10 μm. Results are representative of 10 different fields where at least 50 host cells were visualized.

C. albicans are immunobiologically active and can modulate MO and DC function *in vitro*. Co-incubation with polymyxin B (PMX) did not abrogate NO production (data not shown). In all experiments, lipopolysaccharide (LPS) was used as a positive control with complete inhibition in the presence of PMX (data not shown).

C. albicans-derived *EV reduce fungal burden in an invertebrate model of infection by* C. albicans

As we observed the activation of MO and DC by EV derived from *C. albicans in vitro*, we decided to investigate their biological activity *in vivo* using *G. mellonella* as model. This invertebrate model was established to study cellular and humoural defences with accurate results that correlate with animal models (Hoffmann, 1995; Cotter *et al.*, 2000). The administration of *C. albicans* vesicles with sterol contents corresponding to 1 μM and 2 μM (sterol content) to *G. mellonella* prior to challenge of the larvae with live yeast cells resulted in the significant reduction in fungal CFUs (Fig. 6) and enhanced the survival of the larvae (20% and 40% respectively). Treatment of larvae with EV at higher concentration alone did not cause acute lethality (data not shown).

C. albicans *EV induce up-regulation of the membrane expression of co-stimulatory molecules of MOs and DCs*

The ability of fungal EV to stimulate an adaptive immune response has not been previously reported. To examine this possibility, we evaluated the expression of co-stimulatory molecules such as CD86 and MHC-II by MOs and DC after exposure to *C. albicans* EV. Figure 7A shows that EV-treated MOs displayed a slight increase in CD86 expression (1.2-fold increase). Levels of MHC-II detection were comparable with those of control cells. In contrast, considerably higher levels of CD86 and MHC-II (2.3- and 3.1-fold increase, respectively) were observed in DC exposed to EV in comparison with controls (Fig. 7B).

Discussion

Pathogenic microbes influence disease development by synthesizing and secreting molecules that modulate the immune response. These modulatory effects are usually investigated by minimalistic approaches that include testing of isolated molecules and their targeted host cell receptors. However, during disease initiation and progression, various bioactive molecules are present on the

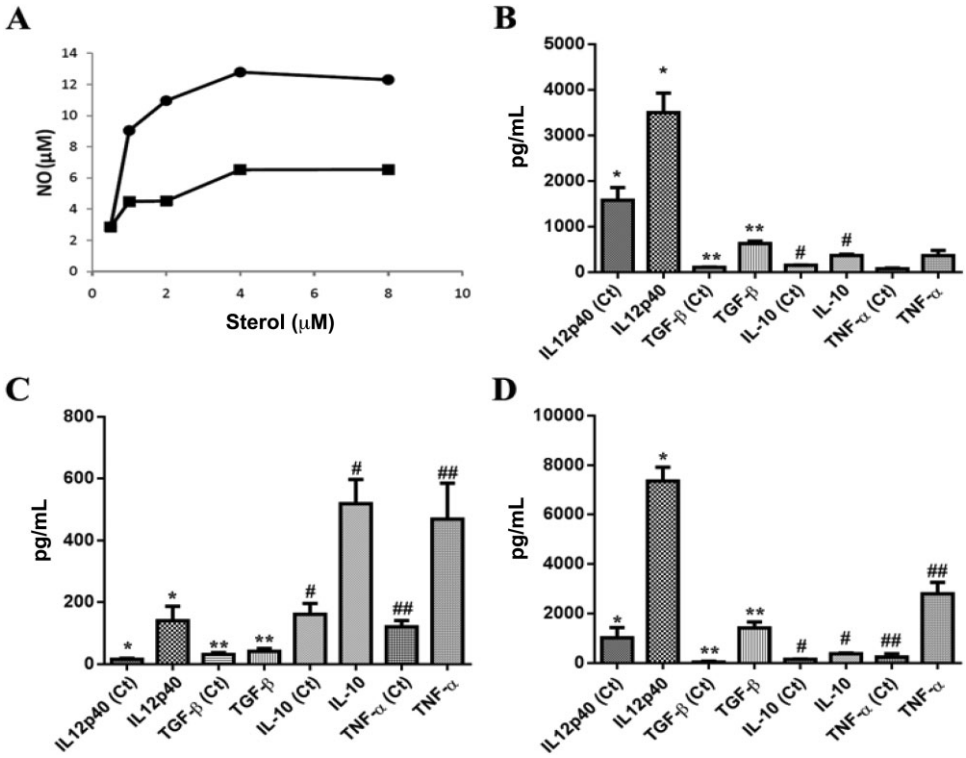

Fig. 5. NO and cytokine production by MOs and DCs stimulated with EV from *C. albicans*. Host cells were stimulated overnight with fungal EV (strain 11) for analysis of NO production and cytokine profiles.
A. Production of NO by MOs (● BM-derived, ■ RAW 264.7) was measured indirectly by Greiss reaction. Production of cytokines (IL-12p40, TGF-β, IL-10 and TNF-α) was measured by capture enzyme-linked immunosorbent assay after incubation of *Candida* vesicles (corresponding to 1 mM of sterol per well) with RAW 264.7 MOs (B), BM-derived MOs (C) and BM-derived DCs (D). Results are representative of three independent experiments. Statistical analysis by Student's *t*-test, $P < 0.05$.

pathogen surface. These molecules, alone or in combination, are usually accessible to host cells. Furthermore, the dynamics of host cell activation is obviously influenced by the viability of the pathogen as immunomodulation profiles resulting from living and killed organisms are usually distinct (O'Leary *et al.*, 2011; Abdullah *et al.*, 2012). These modified patterns of response are directly linked to the secretory activity of living cells, which is required for delivering soluble virulence factors and antigens to the extracellular milieu. Likewise, secreted molecules are not

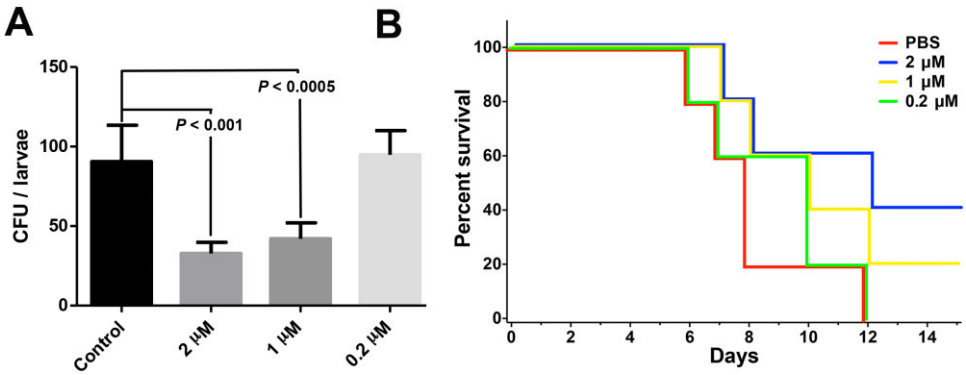

Fig. 6. Protective effect of EV during *G. mellonella* infection with *C. albicans*. *G. mellonella* larvae were inoculated with EV (sterol contents corresponding to 0, 2; 1 and 2 μM) from *C. albicans* (strain 11) 2 days prior to infection with 1×10^6 yeast cells.
A. Fungal survival after *G. mellonella* infection. Larvae were homogenized in PBS 2 days after challenge with *C. albicans* for CFU determination.
B. Survival larvae after infection with yeasts of *C. albicans*. Controls of toxicity included EV-treated larva (2 μM sterol) and larva injected with PBS (not shown). Results are representative of two independent experiments. Statistical analysis by one-way analysis of variance, and the difference between groups were analysed by Bonferroni post test, $P < 0.05$. After day 14 all live larvae turned into pupae.

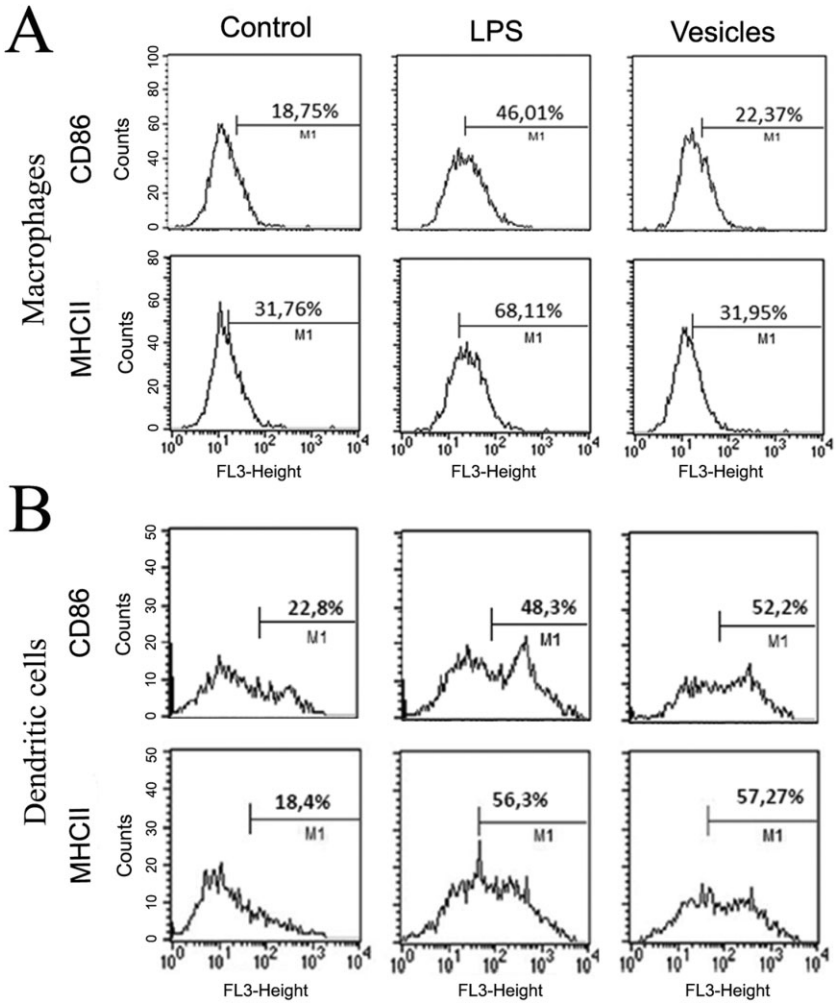

Fig. 7. Surface expression of CD86 and MHC-II by MOs and DCs after exposure to *C. albicans* EV. MOs and DCs were treated overnight with vesicles derived from *C. albicans* strain 11 (1 μM sterol, final concentration). EV-treated cells were incubated with anti-CD86 and anti-MHC-II primary antibodies followed by fluorescent-labelled secondary antibodies. Fluorescence levels were evaluated by flow cytometry.

limited to the site of infection. As extensively described for *C. neoformans* polysaccharides (Dong *et al*., 1999; Barbosa *et al*., 2007; De Jesus *et al*., 2008; Monari *et al*., 2009; Grechi *et al*., 2011), secreted molecules can act distally, impacting the functions of cells and tissues that are not accessible to pathogenic microbes. In fact, for diverse pathogens, secretory ability is correlated with virulence (Puccia *et al*., 1986; Barbosa *et al*., 2007; Dubreuil, 2012; Luo, 2012; Youseff *et al*., 2012). For instance, hydrolytic enzymes are constitutively secreted by *C. albicans* (Naglik *et al*., 2003a; Mayer *et al*., 2013), which is crucial to nutrient acquisition, tissue invasion and damage, and evasion of the host immune response (Naglik *et al*., 2003a). For the reasons listed earlier, we investigated the ability of *C. albicans* to deliver EV-associated molecules to the extracellular environment and consequently modulate immune cells functions.

Release of EV into culture supernatants of bacteria, fungi and protozoa has been investigated in increasing detail in the last 5 years (Rodrigues *et al*., 2007; 2008; Albuquerque *et al*., 2008a; Silverman *et al*., 2008; 2010a; Bomberger *et al*., 2009; Oliveira *et al*., 2009; 2010a; Trocoli Torrecilhas *et al*., 2009; Kaparakis *et al*., 2010; Rivera *et al*., 2010; Roy *et al*., 2010; Chatterjee and Chaudhuri, 2011; Kmetzsch *et al*., 2011; Vallejo *et al*., 2011; 2012a). In fungal pathogens such as *C. neoformans*, *H. capsulatum* and *P. brasiliensis* these vesicles appear responsible for releasing molecules required for virulence and immune modulation (Rodrigues *et al*., 2007; Albuquerque *et al*., 2008a; Vallejo *et al*., 2012a,b). These molecules are distributed into vesicle populations that vary in dimensional and morphological aspects (Albuquerque *et al*., 2008a; Rodrigues *et al*., 2008; Nicola *et al*., 2009; Oliveira *et al*., 2010b; Bayer-Santos *et al*., 2013). In our study, we observed at least two major populations of *C. albicans* EV that were distributed in different size ranges. This specific morphological diversity is corroborated by previous studies (Nicola *et al*., 2009; Oliveira *et al*., 2010b). For instance, EV produced by *S. cerevisiae* are also distributed in two

populations ranging between 40 and 100 nm, and 200 and 500 nm of relative diameter (Oliveira *et al*., 2010b). These data are suggestive of distinct mechanisms of vesicle biogenesis in fungi. According to the literature recently reviewed by Deatherage and Cookson (2012), EV could be formed by budding at the plasma membrane level and/or through multivesicular bodies (MVBs) fusion with the membrane, leading to exosome release. Exosomes range between 50 and 100 nm while shed vesicles are usually larger (Deatherage and Cookson, 2012). MVBs are mature endosomal compartments with multiple luminal invaginations. MVB-like structures have been previously visualized in *C. neoformans* and *S. cerevisiae* (Odorizzi *et al*., 2003; Oliveira *et al*., 2009), and suggested in *C. albicans* (Bruckmann *et al*., 2001). Thus, the two populations observed here are compatible with exosomes (50–100 nm) and budding-derived microvesicles (300–800 nm). The presence of two vesicles populations was demonstrated by Bayer-Santos and colleagues in culture supernatants from the protozoan *Trypanosoma cruzi* (Bayer-Santos *et al*., 2013). Although it would be interesting to understand mechanisms of vesicle biogenesis in fungi, our major goals in the present study included the characterization of vesicle components and their capacity to modulate effective responses in immune cells.

Using chromatographic techniques and tandem mass spectrometry, we identified the major compounds of *C. albicans* EV. Lipid composition in EV from other pathogenic fungal species includes phospholipids, sterol derivatives, and the GSL GlcCer, which are all fundamental components of cellular membranes (Rodrigues *et al*., 2007). Our data indicated that GlcCer and sterols are the principal neutral lipids in EV from *C. albicans*. Notably, GlcCer was recently described as a virulence regulator in *C. neoformans* (Rittershaus *et al*., 2006) and its presence appears to be crucial during disease development and dimorphism in *C. albicans* (Gow *et al*., 2012b). In animal cells, this GSL is associated with addressing proteins to different cellular sites and with hyperacidification of organelles (Sprong *et al*., 2001; van der Poel *et al*., 2011). We speculate that GlcCer can contribute to EV biogenesis and protein addressing. Characterization of EV derived from *C. albicans* lacking GlcCer might reveal additional roles for this GSL during EV formation.

Antigenic proteins were previously detected in EV from *C. neoformans, H. capsulatum* and *P. brasiliensis* (Rodrigues *et al*., 2007; Albuquerque *et al*., 2008a; Vallejo *et al*., 2011). Under the conditions used in our experiments, only two major bands from *C. albicans* EV reacted with serum from patients with candidiasis. However, using silver staining, we visualized several additional bands, suggesting that a more complex protein collection is extracellularly released through EV.

A proteomic analysis of *C. albicans* EV identified 57 unique proteins (Table 1, and Supporting Information Table S1A–D). Notably, a large number of proteins found in EV from *C. albicans* were also characterized in EV from other fungal pathogens (Newport *et al*., 2003; Thomas *et al*., 2009; Vallejo *et al*., 2011; 2012b). A variety of functions have been associated with the majority of these proteins in *C. albicans* and candidiasis, including tissue adhesion and host penetration, biofilm formation, hyphal growth, cell wall organization and modelling, cytokinetic cell separation, heat shock response, evasion of host immune response, glycolytic pathway, metabolism of carbohydrates, lipids and proteins, cell signalling, cell redox homeostasis, nucleoside biosynthesis, cellular response to drugs, peroxidase activity, regulation of DNA replication, regulation of complement activation and proteolysis (see details in Supporting Information Table S2). This complexity is probably derived from the fact that the currently used methods for preparation of fungal vesicles co-isolate compartments of distinct biogenesis. Although many of these proteins have not previously been expected to have surface and/or extracellular distribution, a growing body of evidence confirms that the cell wall is a secondary site for many of these proteins (Long *et al*., 2003; Nimrichter *et al*., 2005; Guimaraes *et al*., 2011; Karkowska-Kuleta *et al*., 2011; Marcos *et al*., 2012). Furthermore, some of these proteins are also found in culture supernatant (Kelly and Kavanagh, 2010). Vesicle transportation could explain the reason by which some nuclear and cytosol proteins are detected in cell wall and culture medium. For instance, proteins such as enolase (Karkowska-Kuleta *et al*., 2011), glyceraldehyde-3-phosphate dehydrogenase (Gpdh) (Gil *et al*., 2006), fructose-bisphosphate aldolase (Pitarch *et al*., 2001), triosephosphate isomerase (Tpi), phosphoglycerate kinase (Pgk) (Karkowska-Kuleta *et al*., 2011) and phosphoglycerate mutase (Crowe *et al*., 2003; Karkowska-Kuleta *et al*., 2011) all play key roles in the glycolytic pathway and are detected at the *C. albicans* cell wall. Notably, enolase, Gpdh, Tpi, Pgk and the glycosyl hydrolase Bgl2, all components of *C. albicans* EV, elicit human antibodies in systemic candidiasis (Pitarch *et al*., 2004). Antibodies to Bgl and enolase are considered biomarkers for a good prognosis in systemic candidiasis (Pitarch *et al*., 2006). According to the literature, other *C. albicans* EV proteins display more than one function, which could be related to their distribution in distinct fungal sites. For example, the mannoprotein MP65 has been characterized as a hydrolase involved with adhesion to endothelial cells, biofilm formation and cell wall integrity (Sandini *et al*., 2011). Finally, it has been recently suggested that fungal EV might correspond to cytoplasmic subtractions derived from plasma membrane

reshaping (Rodrigues *et al*., 2013), which is in agreement with the presence of multiple cytoplasmic proteins in fungal EV.

Fungal EV could affect disease pathogenesis by interacting with and/or delivering their cargo within host cells, as consistently demonstrated for bacterial pathogens. We demonstrated previously that EV from *C. neoformans* are internalized by MOs in a process that does not appear to involve membrane fusion (Oliveira *et al*., 2010a). *Leishmania* EV are delivered to the intracellular environment of MOs (Silverman *et al*., 2010a). On the other hand, Huang and colleagues demonstrated recently that EV from *C. neoformans* fuse with human brain microvascular endothelial cells (HBMECs) membranes (Huang *et al*., 2012). This association is followed by higher indices of adhesion to and traversal of blood–brain barrier by *C. neoformans* yeasts, potentiating brain invasion and meningoencephalitis. Here we demonstrated that EV produced by *C. albicans* were internalized by MOs and DCs within 15 min of incubation. Internalization of *Candida* vesicles appears to involve lipid rafts, as co-localization of vesicles and host cell GM1, a raft marker (Naslavsky *et al*., 1997), was observed. After internalization, EV apparently accumulate at specific subcellular regions, which remain to be accurately determined. Our results were not indicative of membrane fusion as DiC18 was not detected at the host cell plasma membrane after vesicle internalization. In addition, intracellular co-localization of GM1 with EV was visualized, suggesting endosome formation and receptor-mediated internalization. Exosomes from mammalian cells are internalized through endocytosis and transported to perinuclear region (Tian *et al*., 2010). As we did not observe perinuclear accumulation of *C. albicans* vesicles, we speculate that different mechanisms of internalization are involved in this model.

Components of outer membrane vesicles (OMVs) of bacteria and of protozoan EV are detected within host cells, resulting in modulation of their homeostasis (Bomberger *et al*., 2009; Kaparakis *et al*., 2010; Oliveira *et al*., 2010b; Rivera *et al*., 2010; Roy *et al*., 2010; Silverman *et al*., 2010a; Vallejo *et al*., 2011; Huang *et al*., 2012). Some bacterial OMVs also appear to interact with host cells through lipid rafts followed by membrane fusion or receptor-mediated endocytosis (Bomberger *et al*., 2009; Kaparakis *et al*., 2010). As observed in a number of studies using *C. neoformans*, protozoan and bacterial EV, vesicles from *C. albicans* also modulate the effective response of immune cells. Exposure of MOs to *C. albicans* EV resulted in NO production and release of IL-12, IL-10, TGF-β and TNF-α. Notably, the responses of primary cells and RAW 264.7 MOs were not equivalent, which is consistent with the well-known different properties of the activation profiles of primary phagocytes and cell lineages (Jones *et al*., 1983; Momose *et al*., 2000). DCs were also modulated by *C. albicans* EV. Higher amounts of inflammatory cytokines, such as IL-12p40 and TNF-α were detected. However, as observed for MOs, TGF-β and IL-10 synthesis were also increased in DCs when compared with controls. These data corroborate our previous studies using EV from *C. neoformans* and MOs (Oliveira *et al*., 2010a).

Given the experience with other MVs, we expected that EV from *C. albicans* were capable of modulating the innate immune response *in vivo*. According to the recent literature, *G. mellonella* appears to be an ideal model to investigate humoural and innate immune responses in fungal infections (Hoffmann, 1995; Cotter *et al*., 2000). This invertebrate produces six distinct haemocytes and the major antifungal activity is correlated with phagocytosis and oxidative burst (Bergin *et al*., 2005). The decrease in larvae fungal burden after inoculation with EV suggests that these compartments prime the immune response of *G. mellonella*, confirming their capacity to modulate innate immune response. However, under the conditions used in our experiments, treatment with EV did not result in survival differences.

The capacity of EV to activate phagocytic cells led us to investigate their ability to induce expression of co-stimulatory molecules. Our results demonstrated that activation of DC by EV is accompanied by an increase of CD86 and MHC-II expression, suggesting that, similar to *Leishmania* exosomes, these EV could also modulate the adaptive immune response (Silverman *et al*., 2010b). This observation could be related to the most abundant component of *C. albicans* EV, the MP65 mannoprotein. MP65 is a major target for human T-cells, inducing a protective Th1 response (Nisini *et al*., 2001). In addition, this glycoprotein is an efficient inducer of the expression of CD86 and MHC-II and other co-stimulatory molecules in DC (Pietrella *et al*., 2006). Notably, MP65 shares antigenic properties with mannoproteins from *C. neoformans* that induce a protective response during murine challenges with *C. albicans* and *C. neoformans* (Pietrella *et al*., 2002). The complex composition of fungal EV could explain our data, but additional experiments *in vivo* must be performed to better understand their activity during fungal infections. In addition, this observation supports the future exploration of EV in vaccine preparations against fungal infections.

Taken together, our results demonstrate that *C. albicans* EV are immunologically active. In this context, it is reasonable to conclude that these complex membrane compartments have the potential to interfere with the course of candidiasis and other fungal infections, as previously demonstrated for *C. neoformans* (Kmetzsch *et al*., 2011). Because of their complex molecular composition, it is impossible to predict whether *C. albicans* EV would enhance fungal pathogenesis or stimulate disease

control in mammalian invasive disease conditions, outcomes that cannot be distinguished at this time from the data available. Our findings show that *C. albicans* EV are structurally complex and immunologically active and thus provide a fertile area for future investigations of their role in pathogenesis.

Experimental procedures

Fungal strains and growth conditions

Three strains of *C. albicans* (ATCC 90028, ATCC SC5314 and 11) were used. Strain 11 was isolated from a male patient at Institute of Hematology Arthur Siqueira Cavalcanti and kindly provided by Dr Dornelas (Braga-Silva *et al.*, 2009; Laboratory Microbiology and Mycology – HemoRio). *C. albicans* yeast cells were cultivated in liquid Sabouraud medium for 48 h at 30°C with shaking (150 rpm).

EV isolation

EVs were isolated from *C. albicans* conditioned medium, as described (Rodrigues *et al.*, 2007). In brief, *C. albicans* supernatants from 48 h cultures were subjected to sequential centrifugation steps (4000 and 15 000× g, 15 min, at 4°C). Remaining yeasts and debris were removed by an additional step of supernatant filtration using a 0.8 μm membrane filter (Merck Millipore). Cell-free supernatants were then concentrated approximately 20-fold using an Amicon ultrafiltration system (cut-off, 100 kDa, Millipore) and then centrifuged at 100 000× g for 1 h at 4°C. Supernatants were then discarded and EV-containing pellets washed twice with 0.1 M phosphate-buffered saline (PBS) pH 7.4 at 100 000× g for 1 h at 4°C.

Mammalian cells

LPS-free conditions were used to cultivate all host cells used in this study. The murine MO cell line RAW 264.7 (ATCC, Manassas) was grown in DMEM (Invitrogen, Life Technologies) supplemented with 10% foetal calf serum, 2 mM L-glutamine, 1 mM pyruvate sodium, 10 mg ml^{-1} gentamicin, 10 mM minimal essential medium (MEM) non-essential amino acids, 10 mM N-2-hydroxyethylpiperazine-N′-2-ethanesulfonic acid, and 50 mM 2-mercaptoethanol (β-ME) at 37°C and 5% CO_2. BM-derived cells from 4 to 12 weeks old Bagg albino (BALB)/c mice were used to generate MO and DCs according to (Stanley and Heard, 1977; Lutz *et al.*, 1999).

Animals

The use of mice was approved by the institutional Animal Care and Use Committee of the Federal University of Rio de Janeiro. BM-derived cells from 4 to 12 weeks old BALB/c mice were used to generate MOs and DC according to (Stanley and Heard, 1977; Lutz *et al.*, 1999). For BM-derived MO, 2×10^6 BM-derived cells were cultivated in RPMI 1640 medium supplemented with 2 mM L-glutamine, 1 mM sodium pyruvate, 10 mM MEM non-essential amino acids, 50 μM β-ME and 20 ng ml^{-1} rM – colony stimulating factor (CSF MO) at 37°C and 5% CO_2. Factor rM – CSF (20 ng ml^{-1}) was added each third day of culture, replacing one-third of the culture medium. BM-derived DC were obtained after 10 days under similar conditions, but in the presence of recombinant granulocyte-MO CSF (*rGM-CSF*, Peprotech) 20 ng mL^{-1} as factor. Cell cultures were stained for DC with CD11c-FITC (eBioscience) and MO with F4/80-FITC or PercP.Cy5.5 (eBioscience).

TEM

Transmission electron microscopy was used to visualize intact *C. albicans* yeast cells and EV. The pellets containing *C. albicans* were fixed in 2% glutaraldehyde in 0.1 M cacodylate at room temperature for 2 h and then incubated overnight in 4% formaldehyde, 1% glutaraldehyde and 0.1 M PBS. Samples were incubated for 90 min in 2% osmium, serially dehydrated in ethanol (30%, 50%, 70% plus uranyl 5% H_2O, 90%, 100% 2×), and embedded in Spurr's epoxy resin. Thin sections were obtained on a Reichert Ultracut and stained with 0.5% uranyl acetate and 0.5% lead citrate. Samples were observed in a JEOL 1200EX transmission electron microscope operating at 80 kV (Rodrigues *et al.*, 2007; Albuquerque *et al.*, 2008a). To visualize vesicles isolated from culture supernatants of *C. albicans*, samples were fixed in 2.5% glutaraldehyde in 0.1 M cacodylate buffer at room temperature for 2 h and then incubated overnight in 4% paraformaldehyde, 1% glutaraldehyde and 0.1 M PBS. Samples were then incubated for 90 min in 2% osmium tetroxide, serially dehydrated in ethanol and embedded in Spurr's epoxy resin. Thin sections were obtained on a Reichert Ultracut and stained with 0.5% uranyl acetate and 0.5% lead citrate. Samples were observed in a JEOL 1200EX transmission electron microscope (JEOL, Ltd.), operating at 80 kV (Albuquerque *et al.*, 2008b).

Lipid analysis

Otherwise indicated, all reagents and solvents used for lipid analysis were of the highest grade available and were acquired from Sigma-Aldrich. EV were suspended in a mixture of chloroform ($CHCl_3$) : methanol (MeOH) : water (H_2O) (8:4:3, v/v/v). The mixture was vigorously vortexed and then centrifuged to discard precipitates. Water was added to achieve a ratio of $CHCl_3$: MeOH : H_2O (8:4:5.6, v/v/v) and a two-phase system was obtained (Schnaar, 1994). The lower phase containing neutral lipids (sterol-enriched) was dried under N_2 atmosphere and then dissolved in 50 μl of MeOH. Aliquots of 5–10 μl were analysed by HPTLC. For sterol analysis, the lipid extract was loaded into HPTLC silica plates (Merck) and resolved using a solvent system containing hexane : ether : acetic acid (80:40:2, v/v/v) solvent. The plate was then sprayed with a solution of 50 mg ferric chloride ($FeCl_3$) in a mixture of 90 ml water, 5 ml acetic acid and 5 ml sulfuric acid. Sterols were visualized as red-violet spots after heating at 100°C for 3–5 min (Rodrigues *et al.*, 2007). GlcCer was resolved using $CHCl_3$: MeOH : H_2O (65:25:4, v/v/v) (Folch *et al.*, 1957) and visualized after spraying with orcinol-sulfuric acid reagent, followed by heating at 150°C for 5 min (Barreto-Bergter *et al.*, 2004). All experiments were performed in triplicate and the results analysed by Student's *t*-test.

SDS-PAGE and immunoblotting analysis

Proteins from EV preparations were quantified by Bio-Rad Protein Assay Kit (Bio-Rad). The equivalent of 15 μg was

dissolved in loading buffer (1% SDS, 10% glycerol, 10 mM Tris-HCl [pH 6.8], 1 mM β-ME, and 0.05 mg ml^{-1} bromophenol blue) and separated by 12% PAGE. Total protein profile was visualized after impregnation with silver nitrate. In addition, resolved proteins were transferred to nitrocellulose membranes and blocked with 5% fat-free milk in PBS –0.05% Tween 20 (PBS-T) for at least 1 h. Membranes were then incubated individually with anti-SAP 1–3 antibodies (Braga-Silva *et al*., 2009), serum from mice 7 days after intravenous infection with 10^6 *C. albicans* (strain 11) yeast cells (1:500), or 2 μg mL^{-1} biotinylated ConA for 1h at 37°C. After washing three times with PBS-T, membranes were incubated with HRP-conjugated anti-rabbit or anti-mouse IgG (1:2500) or avidin-HRP (1:1000). ECL (Bio-Rad) or 3,3′-diaminobenzidine (DAB, Sigma-Aldrich) solution [5 μg ml^{-1} DAB in 8.8 M H_2O_2 (30%)] were used to develop the immunoblots. Protein extracts from *S. cerevisiae* strain SEY6210 were used as negative control. Culture supernatant from *C. albicans* strain 11 under optimal conditions for SAP secretion was used as positive control (Ruchel *et al*., 1983). All experiments were performed in triplicate.

Dynamic light scattering analysis of EV

The effective diameter of EV preparations was measured by QELS in a 90Plus/BI-MAS Multi Angle Particle Sizing analyser (Brookhaven Instruments Corp.). Measurements were done at 25°C. The multimodal distributions of particle size diameter were generated by a non-negatively constrained least squares algorithm based on the intensity of light scattered by each particle. All experiments were performed in triplicate and analysed under the same conditions.

Proteomic analysis by liquid chromatography-tandem mass spectrometry (LC-MS/MS)

Protein pellets were suspended in 100 μL 0.4 M NH_4HCO_3 containing 8 M urea and reduced with 5 mM dithiolthreitol for 30 min at 55°C. Reduced thiol groups were alkylated with 10 mM iodoacetamide for 30 min at room temperature, and diluted eightfold to a final concentration of 1 M urea, 50 mM NH_4HCO_3. Samples (approx. 10 picomoles of total protein) were digested overnight at 37°C with 6 μg sequencing grade trypsin (Sigma-Aldrich). After quenching the reaction with trifluoroacetic acid (TFA) to a final concentration of 0.05% TFA, samples were desalted on 100-mg C18 cartridges (Supelco, Sigma-Aldrich) and dried in a vacuum centrifuge. Recovered peptides were dissolved in 2% acetonitrile (ACN) 0.5% formic acid (FA) and subjected to 2D LC-MS/MS analysis, using an Eksigent 1D-plus nanoLC coupled to a Thermo Fisher LTQ XL/ETD-MS (Thermo Fisher Scientific), equipped at the front end with a TriVersa NanoMate electrospray ionization nano-source (Advion). The separation was carried out in an in-house 10-cm C18-reverse phase column (360 μm OD, 75 μm I.D., packed with Phenomenex Luna 5 μm C18, 100 Å) (Phenomenex) in a linear gradient (Solvent A: 5% ACN/0.1% FA, Solvent B: 80% ACN/0.1% FA). Peptides were eluted in a linear gradient of 5–40% B over 100 min, following an online salt step fractionation on a 5 μL strong cation exchange SCX column (Optimized Technologies, Inc.) essentially as described (Bayona *et al*., 2011; Nakayasu *et al*., 2012). The MS system was set to perform one full scan (400–1700 *m/z* range) followed by MS/MS of the 10 most abundant parent-ions (isolation width = 3.0 *m/z*; 35 normalized collision energy). The dynamic exclusion was set to collect each parent-ion twice and then excluded for 60 s. Tandem mass spectra derived from peptides with 800–3500 Da, more than 10 counts, and at least 15 fragment ions were converted into DTA files using Bioworks v.3.3.1 (Thermo Fisher Scientific). Peak list in DTA format were searched using TurboSequest (available in Bioworks) against *C. albicans*, available downloaded from Uniprot (http://www.uniprot.org/) on December 2, 2012, human keratin and porcine trypsin sequences from the GenBank (http://www.ncbi.nlm.nih.gov/genbank/), in both correct (forward) and reversed orientations forming a database with 34 494 sequences. Because of sample amount limitation, we were only able to perform a single 2D LC-MS/MS proteomic analysis of each biological sample. Under these circumstances, the 2D LC-MS/MS analysis provided the best peptide/protein identification coverage. All LC-MS/MS raw files were deposited at PeptideAtlas repository and are available for download at http://www.peptideatlas.org/PASS/PASS00303.

Database search parameters included: (i) fully tryptic peptides with one missed cleavage site allowed, (ii) cysteine carbamidomethylation as a fixed modification, (iii) methionine oxidation as a variable modification and (iv) 2 Da and 1 Da for peptide and fragment mass tolerance respectively. TurboSequest outputs were filtered with DCn ≥ 0.05, peptide probability ≤ 0.05, and Xcorr ≥ 1.5, 2.0, and 2.5 for singly-, doubly- and triply charged peptides respectively. After filtering, files were converted into XML format and peptide sequences were assembled into proteins and redundant proteins into protein groups using an in-house written script (Nakayasu *et al*., 2012). A protein group comprises at least one protein that is identified by a set of peptides that, collectively, are not included in other protein group. To ensure a false-discovery rate smaller than 1% proteins were filtered with XCorr sum ≥ 3.0.

Vesicle quantification

The quantification of EV fractions was determined based on the presence of sterols, using the quantitative fluorimetric kit 'Amplex Red Sterol Assay Kit' (Molecular Probes, Life Technologies) or phospholipids, using the 'EnzyChromTM Phospholipid Assay Kit' (EPLP-100, BioAssay Systems).

Cell viability

RAW 264.7 MO and BM-derived cells (MO and DC) were plated onto 96-well plates (10^5 cells per well) and incubated with different concentrations of EV based on sterol content (0.5–2 μM) for 16 h. Supernatants were then collected and lactate dehydrogenase (LDH) activity was measured. LDH is a cytoplasmic enzyme retained by viable cells with intact plasma membranes. Membrane damage results in LDH release and its accumulation in the supernatant. Aliquots (80 μL) of supernatant were mixed with a buffer reaction (PBS containing 0.7 mM NADH and 4.7 mM pyruvate). Consumption of NADH, proportional to LDH activity, was measured in a spectrophotometer (Δ340 nm). Positive and negative controls consist, respectively, of host cells lysed with triton X-100 and supernatant of untreated cells after 16 h of cultivation. All experiments were performed in triplicate and the results analysed by Student's *t*-test.

Production of NO

RAW 264.7 and BM-derived MO were plated onto 96-well plates (10^5 per well) and washed twice with serum-free DMEM. Host cells were then treated overnight in RPMI with EV from *C. albicans* (strain 11) at different concentrations (0.5, 1, 2, 4 and 8 μM sterol per well). LPS from *Escherichia coli* (Sigma-Aldrich, 1 μg ml^{-1}) was used as positive control. NO was measured by Griess method (Green *et al*., 1982). PMX (40 μg ml^{-1}, Sigma-Aldrich) was added to the wells to exclude the possibility of LPS contamination. All experiments were performed in triplicate sets and statistically analysed by using Student's *t*-test.

Production of cytokines by MOs and DCs after stimulation of vesicles

RAW 264.7 and BM-derived cells (MO and DC) were plated onto 24-well plates (5×10^5 cells per well) and incubated with EV from *C. albicans* strain 11 (1 μM sterol per well) for 24 h in the presence of 1% v/v Nutridoma-SP (Boehringer Mannheim Biochemical, Roche Applied Science) at 37°C and 5% CO_2. *E. coli* LPS (1 μg ml^{-1}) was used as positive control. The supernatants were collected and IL-10, IL-12p40, TGF-β and TNF-α concentrations were determined by enzyme-linked immunosorbent assay according to the manufacturer's protocol (R&D Systems). (Decote-Ricardo *et al*., 2009; Oliveira *et al*., 2010a). All experiments were performed in triplicate and the results analysed by Student's *t*-test.

Expression of co-stimulatory molecules

RAW 264.7 and BM-derived cells were plated onto six-well plates (3×10^6 cells per well) and incubated with EV from *C. albicans* strain 11 (1 μM of sterol per well) for 24 h at 37°C and 5% CO_2. Expression of MHC-II and CD86 was analysed by flow cytometry. The cells were collected and labelled with FITC anti-CD11c, anti-PE IAD (MHC-II) and anti-CD86 PECy5 antibodies for 30 min at 4°C. The antibodies dilutions were used according to the manufacturer's recommendations (eBioscience). The cells were then washed and fixed with 4% paraformaldehyde (Sigma-Aldrich) and analysed in a FACScalibur (BD Biosciences). The results were analysed using CellQuest program (BD Biosciences) (Decote-Ricardo *et al*., 2009). *E. coli* LPS (100 ng mL^{-1}) was used as positive control. All experiments were performed in triplicates and the results analysed by Student's *t*-test.

Internalization of EV by host cells

RAW 264.7 and BM-derived cells (MO an DC) were plated onto 24-well plates covered with sterile glass coverslips (5×10^5 cells per well) and incubated with EV from *C. albicans* strain 11 (1 μM sterol per well) for different time points (5, 15 and 60 min and overnight) at 37°C and 5% CO_2 atmosphere (Oliveira *et al*., 2010a). EV used in these experiments were previously stained with 3 mM $DiIC_{18}$ (Invitrogen), a fluorescent lipophilic compound that intercalates cell membranes (Oliveira *et al*., 2010a). $DiIC_{18}$ incubated with PBS under the same conditions was used as negative control. After the incubation period, host cells were washed with PBS and fixed with 4% PF for 30 min at room temperature. Cells were then washed and blocked with PBS/BSA1% for 1 h at room temperature. The fluorescence intensity of MOs and DCs is a direct function of the components associated with $DiIC_{18}$-labelled vesicles. After fixation with 4% paraformaldehyde (PF), cells were washed and labelled with cholera toxin subunit B (CtxB) (1 μg ml^{-1}) and 4,6-diamidino-2-phenylindole (DAPI) (10 μg ml^{-1}), respectively, as described (Vyas *et al*., 2001; Oliveira *et al*., 2010a). The slides were then washed three times with PBS and mounted in 50% glycerol and 50 mM n-propyl gallate in PBS. The slides were visualized with an AxioVision 4.8. (Carl Zeiss International) microscope. Fluorescence confocal microscopy images were then collected using an LSM 510 META NLO confocal microscope (Carl Zeiss International). Excitation of DAPI-labelled cell nuclei was achieved by two-photon excitation regime using a Mai Tai HP pulsed infrared laser (Spectra-Physics, Lasers) at 740 nm. FITC-labelled CtxB and $DiIC_{18}$ labelled vesicles were excited with argon ion laser at 488 nm and a diode laser at 561 nm respectively. Emissions were collected separated in three channels using bandpass filters BP 435–485 IR (blue channel), BP 500–550 IR (green channel) and BP 575–615 IR (red channel). All confocal microscopy images were collected using a Plan-Apochromat 63×/1.4 DIC M27 oil immersion objective. Pinhole diameters were set to 1 Airy unit corresponding to a z resolution of 0.8 μm.

G. mellonella *survival and fungal burden assays*

Galleria mellonella larvae in the final instar larval stage were selected according to similarity in size and weight (0.10–0.15 g). Larvae (15 per group) were inoculated with 10 μl of EV suspensions (0, 2, 1 or 2 μM per insect, according to phospholipid quantification) with a Hamilton syringe into the haemocoel through the last proleg as described by Brennan *et al*. (2002). The same number of caterpillars was inoculated with PBS in each experiment to monitor potential effects because of physical injury and a second control group was caterpillars without any manipulation. All larvae were placed in sterile Petri dishes and maintained in the dark at 37°C in a stationary incubator. Two days later, all larvae were inoculated with 10 μl of a suspension containing 1×10^6 of *C. albicans* (strain 11). Controls of toxicity included EV (2 μM) treated larva and larva injected with PBS. Larva mortality was monitored daily. Larva death was assessed by the lack of movement in response to stimulation. Killing curves were plotted and statistical analyses were performed using the log–rank (Mantel–Cox) test survival GraphPad Prism 5 and results represent the mean percentage survival of larvae from all assays. Two days after infection, five inoculated larvae were homogenized in 2 ml PBS and 100 μl aliquots of this solution were plated on yeast extract-peptone-dextrose agar (Difco Bacto) containing 0.1% and 1% penicillin/streptomycin (Gibco-BRL/Life Technologies) to prevent bacterial growth and plates were incubated at 30°C.

Acknowledgements

L.N., G.V. and M.L.R. are supported by grants from the Brazilian agencies Fundação de Amparo à Pesquisa do Estado do Rio de Janeiro (FAPERJ), Conselho Nacional de Desenvolvimento Científico e Tecnológico (CNPq), Coordenação

de Aperfeiçoamento de Pessoal de Nível Superior (CAPES) and in part by Fundação de Amparo a Pesquisa do Estado de São Paulo (FAPESP). J.D.N. is supported in part by an Irma T. Hirschl/Monique Weill-Caulier Trust Research Award. I.C.A. is partly supported by the National Institutes of Health grant no. 2G12MD007592 (to BBRC/UTEP). J.D.N. and I.C.A. are special visiting-researcher fellows of the Science Without Borders Program, CNPq-Brazil. We are grateful to the Biomolecule Analysis Core Facility (BACF) at the Border Biomedical Research Center (BBRC), University of Texas at El Paso (UTEP) for the access to the LC-MS instrument used in this study. BACF is supported by the Research Centers in Minority Institutions (RCMI) program, grant 2G12MD007592, 2G12RR008124-16A1, and 2G12RR008124-16A1S1, to the Border Biomedical Research Center (BBRC) at UTEP, from the National Institutes on Minority Health and Health Disparities (NIMHD), a component of the NIH.

References

Abdullah, Z., Schlee, M., Roth, S., Mraheil, M.A., Barchet, W., Bottcher, J., *et al*. (2012) RIG-I detects infection with live *Listeria* by sensing secreted bacterial nucleic acids. *EMBO J* **31:** 4153–4164.

Albuquerque, P.C., Nakayasu, E.S., Rodrigues, M.L., Frases, S., Casadevall, A., Zancope-Oliveira, R.M., *et al*. (2008a) Vesicular transport in *Histoplasma capsulatum*: an effective mechanism for trans-cell wall transfer of proteins and lipids in ascomycetes. *Cell Microbiol* **10:** 1695–1710.

Albuquerque, P.C., Nakayasu, E.S., Rodrigues, M.L., Frases, S., Casadevall, A., Zancope-Oliveira, R.M., *et al*. (2008b) Vesicular transport in *Histoplasma capsulatum*: an effective mechanism for trans-cell wall transfer of proteins and lipids in ascomycetes. *Cell Microbiol* **10:** 1695–1710.

Anderson, J., Mihalik, R., and Soll, D.R. (1990) Ultrastructure and antigenicity of the unique cell wall pimple of the *Candida* opaque phenotype. *J Bacteriol* **172:** 224–235.

Arendrup, M.C. (2010) Epidemiology of invasive candidiasis. *Curr Opin Crit Care* **16:** 445–452.

Azie, N., Neofytos, D., Pfaller, M., Meier-Kriesche, H.U., Quan, S.P., and Horn, D. (2012) The PATH (Prospective Antifungal Therapy) Alliance(R) registry and invasive fungal infections: update 2012. *Diagn Microbiol Infect Dis* **73:** 293–300.

Barbosa, F.M., Fonseca, F.L., Figueiredo, R.T., Bozza, M.T., Casadevall, A., Nimrichter, L., and Rodrigues, M.L. (2007) Binding of glucuronoxylomannan to the CD14 receptor in human A549 alveolar cells induces interleukin-8 production. *Clin Vaccine Immunol* **14:** 94–98.

Barreto-Bergter, E., Pinto, M.R., and Rodrigues, M.L. (2004) Structure and biological functions of fungal cerebrosides. *An Acad Bras Cienc* **76:** 67–84.

Batanghari, J.W., Deepe, G.S., Jr, Di Cera, E., and Goldman, W.E. (1998) Histoplasma acquisition of calcium and expression of CBP1 during intracellular parasitism. *Mol Microbiol* **27:** 531–539.

Bayer-Santos, E., Aguilar-Bonavides, C., Rodrigues, S.P., Cordero, E.M., Marques, A.F., Varela-Ramirez, A., *et al*. (2013) Proteomic analysis of *Trypanosoma cruzi* secretome: characterization of two populations of extracellular vesicles and soluble proteins. *J Proteome Res* **12:** 883–897.

Bayona, J.C., Nakayasu, E.S., Laverriere, M., Aguilar, C., Sobreira, T.J., Choi, H., *et al*. (2011) SUMOylation pathway in *Trypanosoma cruzi*: functional characterization and proteomic analysis of target proteins. *Mol Cell Proteomics* **10** (M110)**:** 007369.

Bergin, D., Reeves, E.P., Renwick, J., Wientjes, F.B., and Kavanagh, K. (2005) Superoxide production in *Galleria mellonella* hemocytes: identification of proteins homologous to the NADPH oxidase complex of human neutrophils. *Infect Immun* **73:** 4161–4170.

Bomberger, J.M., Maceachran, D.P., Coutermarsh, B.A., Ye, S., O'Toole, G.A., and Stanton, B.A. (2009) Long-distance delivery of bacterial virulence factors by *Pseudomonas aeruginosa* outer membrane vesicles. *PLoS Pathog* **5:** e1000382.

Braga-Silva, L.A., and Santos, A.L. (2011) Aspartic protease inhibitors as potential anti-*Candida albicans* drugs: impacts on fungal biology, virulence and pathogenesis. *Curr Med Chem* **18:** 2401–2419.

Braga-Silva, L.A., Mesquita, D.G., Ribeiro, M.D., Carvalho, S.M., Fracalanzza, S.E., and Santos, A.L. (2009) Trailing end-point phenotype antibiotic-sensitive strains of *Candida albicans* produce different amounts of aspartyl peptidases. *Br J Med Biol Res* **42:** 765–770.

Brennan, M., Thomas, D.Y., Whiteway, M., and Kavanagh, K. (2002) Correlation between virulence of *Candida albicans* mutants in mice and *Galleria mellonella* larvae. *FEMS Immunol Med Microbiol* **34:** 153–157.

Bruckmann, A., Kunkel, W., Augsten, K., Wetzker, R., and Eck, R. (2001) The deletion of CaVPS34 in the human pathogenic yeast *Candida albicans* causes defects in vesicle-mediated protein sorting and nuclear segregation. *Yeast* **18:** 343–353.

Calderone, R., and Wadsworth, E. (1987) Characterization with crossed immunoelectrophoresis of some antigens differentiating a virulent *Candida albicans* from its derived, avirulent strain. *Proc Soc Exp Biol Med* **185:** 325–334.

Chatterjee, D., and Chaudhuri, K. (2011) Association of cholera toxin with *Vibrio cholerae* outer membrane vesicles which are internalized by human intestinal epithelial cells. *FEBS Lett* **585:** 1357–1362.

Cheng, S.C., Joosten, L.A., Kullberg, B.J., and Netea, M.G. (2012) Interplay between *Candida albicans* and the mammalian innate host defense. *Infect Immun* **80:** 1304–1313.

Concia, E., Azzini, A.M., and Conti, M. (2009) Epidemiology, incidence and risk factors for invasive candidiasis in high-risk patients. *Drugs* **69** (Suppl. 1)**:** 5–14.

Cotter, G., Doyle, S., and Kavanagh, K. (2000) Development of an insect model for the *in vivo* pathogenicity testing of yeasts. *FEMS Immunol Med Microbiol* **27:** 163–169.

Crowe, J.D., Sievwright, I.K., Auld, G.C., Moore, N.R., Gow, N.A., and Booth, N.A. (2003) *Candida albicans* binds human plasminogen: identification of eight plasminogen-binding proteins. *Mol Microbiol* **47:** 1637–1651.

De Jesus, M., Park, C.G., Su, Y., Goldman, D.L., Steinman, R.M., and Casadevall, A. (2008) Spleen deposition of

Cryptococcus neoformans capsular glucuronoxylomannan in rodents occurs in red pulp macrophages and not marginal zone macrophages expressing the C-type lectin SIGN-R1. *Med Mycol* **46:** 153–162.

Deatherage, B.L., and Cookson, B.T. (2012) Membrane vesicle release in bacteria, eukaryotes, and archaea: a conserved yet underappreciated aspect of microbial life. *Infect Immun* **80:** 1948–1957.

Decote-Ricardo, D., Chagas, K.K., Rocha, J.D., Redner, P., Lopes, U.G., Cambier, J.C., *et al*. (2009) Modulation of *in vitro* murine B-lymphocyte response by curcumin. *Phytomedicine* **16:** 982–988.

Dong, Z.M., Jackson, L., and Murphy, J.W. (1999) Mechanisms for induction of L-selectin loss from T lymphocytes by a cryptococcal polysaccharide, glucuronoxylomannan. *Infect Immun* **67:** 220–229.

Dubreuil, J.D. (2012) The whole Shebang: the gastrointestinal tract, *Escherichia coli* enterotoxins and secretion. *Curr Issues Mol Biol* **14:** 71–82.

Eisenman, H.C., Frases, S., Nicola, A.M., Rodrigues, M.L., and Casadevall, A. (2009) Vesicle-associated melanization in *Cryptococcus neoformans*. *Microbiology* **155:** 3860–3867.

Folch, J., Lees, M., and Sloane Stanley, G.H. (1957) A simple method for the isolation and purification of total lipides from animal tissues. *J Biol Chem* **226:** 497–509.

Gacser, A., Stehr, F., Kroger, C., Kredics, L., Schafer, W., and Nosanchuk, J.D. (2007) Lipase 8 affects the pathogenesis of *Candida albicans*. *Infect Immun* **75:** 4710–4718.

Gehrmann, U., Qazi, K.R., Johansson, C., Hultenby, K., Karlsson, M., Lundeberg, L., *et al*. (2011) Nanovesicles from *Malassezia sympodialis* and host exosomes induce cytokine responses – novel mechanisms for host-microbe interactions in atopic eczema. *PLoS ONE* **6:** e21480.

Gil, M.L., Dagan, S., Eren, R., and Gozalbo, D. (2006) Evaluation of the usefulness of anti-glyceraldehyde-3-phosphate dehydrogenase antibodies as a treatment for invasive candidiasis in a murine model. *Antonie Van Leeuwenhoek* **89:** 345–350.

Gow, N.A., and Hube, B. (2012a) Importance of the *Candida albicans* cell wall during commensalism and infection. *Curr Opin Microbiol* **15:** 406–412.

Gow, N.A., van de Veerdonk, F.L., Brown, A.J., and Netea, M.G. (2012b) *Candida albicans* morphogenesis and host defence: discriminating invasion from colonization. *Nat Rev Microbiol* **10:** 112–122.

Grechi, J., Marinho-Carvalho, M., Zancan, P., Cinelli, L.P., Gomes, A.M., Rodrigues, M.L., *et al*. (2011) Glucuronoxylomannan from *Cryptococcus neoformans* down-regulates the enzyme 6-phosphofructo-1-kinase of macrophages. *J Biol Chem* **286:** 14820–14829.

Green, L.C., Wagner, D.A., Glogowski, J., Skipper, P.L., Wishnok, J.S., and Tannenbaum, S.R. (1982) Analysis of nitrate, nitrite, and [15N]nitrate in biological fluids. *Anal Biochem* **126:** 131–138.

Guimaraes, A.J., Nakayasu, E.S., Sobreira, T.J., Cordero, R.J., Nimrichter, L., Almeida, I.C., and Nosanchuk, J.D. (2011) *Histoplasma capsulatum* heat-shock 60 orchestrates the adaptation of the fungus to temperature stress. *PLoS ONE* **6:** e14660.

Hazen, K.C. (1995) New and emerging yeast pathogens. *Clin Microbiol Rev* **8:** 462–478.

Heinsbroek, S.E., Brown, G.D., and Gordon, S. (2005) Dectin-1 escape by fungal dimorphism. *Trends Immunol* **26:** 352–354.

Hoffmann, J.A. (1995) Innate immunity of insects. *Curr Opin Immunol* **7:** 4–10.

Huang, S.H., Wu, C.H., Chang, Y.C., Kwon-Chung, K.J., Brown, R.J., and Jong, A. (2012) *Cryptococcus neoformans*-derived microvesicles enhance the pathogenesis of fungal brain infection. *PLoS ONE* **7:** e48570.

Jones, C.M., Goldfarb, R.H., and Holden, H.T. (1983) Macrophage cell lines behave as activated macrophages in the production and regulation of plasminogen activator. *Cancer Invest* **1:** 207–213.

Jouault, T., Sarazin, A., Martinez-Esparza, M., Fradin, C., Sendid, B., and Poulain, D. (2009) Host responses to a versatile commensal: PAMPs and PRRs interplay leading to tolerance or infection by *Candida albicans*. *Cell Microbiol* **11:** 1007–1015.

Kaparakis, M., Turnbull, L., Carneiro, L., Firth, S., Coleman, H.A., Parkington, H.C., *et al*. (2010) Bacterial membrane vesicles deliver peptidoglycan to NOD1 in epithelial cells. *Cell Microbiol* **12:** 372–385.

Karkowska-Kuleta, J., Kedracka-Krok, S., Rapala-Kozik, M., Kamysz, W., Bielinska, S., Karafova, A., and Kozik, A. (2011) Molecular determinants of the interaction between human high molecular weight kininogen and *Candida albicans* cell wall: identification of kininogen-binding proteins on fungal cell wall and mapping the cell wall-binding regions on kininogen molecule. *Peptides* **32:** 2488–2496.

Kelly, J., and Kavanagh, K. (2010) Proteomic analysis of proteins released from growth-arrested *Candida albicans* following exposure to caspofungin. *Med Mycol* **48:** 598–605.

Kim, J., and Sudbery, P. (2011) *Candida albicans*, a major human fungal pathogen. *J Microbiol* **49:** 171–177.

Kmetzsch, L., Joffe, L.S., Staats, C.C., de Oliveira, D.L., Fonseca, F.L., Cordero, R.J., *et al*. (2011) Role for Golgi reassembly and stacking protein (GRASP) in polysaccharide secretion and fungal virulence. *Mol Microbiol* **81:** 206–218.

Kuehn, M.J., and Kesty, N.C. (2005) Bacterial outer membrane vesicles and the host–pathogen interaction. *Genes Dev* **19:** 2645–2655.

Long, K.H., Gomez, F.J., Morris, R.E., and Newman, S.L. (2003) Identification of heat shock protein 60 as the ligand on *Histoplasma capsulatum* that mediates binding to CD18 receptors on human macrophages. *J Immunol* **170:** 487–494.

Lopez-Ribot, J.L., Gozalbo, D., Sepulveda, P., Casanova, M., and Martinez, J.P. (1995) Preliminary characterization of the material released to the culture medium by *Candida albicans* yeast and mycelial cells. *Antonie Van Leeuwenhoek* **68:** 195–201.

Luo, Z.Q. (2012) *Legionella* secreted effectors and innate immune responses. *Cell Microbiol* **14:** 19–27.

Lutz, M.B., Kukutsch, N., Ogilvie, A.L., Rossner, S., Koch, F., Romani, N., and Schuler, G. (1999) An advanced culture

method for generating large quantities of highly pure dendritic cells from mouse bone marrow. *J Immunol Methods* **223:** 77–92.

Marcos, C.M., de Fatima da Silva, J., de Oliveira, H.C., Moraes da Silva, R.A., Mendes-Giannini, M.J., and Fusco-Almeida, A.M. (2012) Surface-expressed enolase contributes to the adhesion of *Paracoccidioides brasiliensis* to host cells. *FEMS Yeast Res* **12:** 557–570.

Mayer, F.L., Wilson, D., and Hube, B. (2013) *Candida albicans* pathogenicity mechanisms. *Virulence* **4:** 119–128.

Momose, I., Terashima, M., Nakashima, Y., Sakamoto, M., Ishino, H., Nabika, T., *et al*. (2000) Phorbol ester synergistically increases interferon regulatory factor-1 and inducible nitric oxide synthase induction in interferon-gamma-treated RAW 264.7 cells. *Biochim Biophys Acta* **1498:** 19–31.

Monari, C., Bevilacqua, S., Piccioni, M., Pericolini, E., Perito, S., Calvitti, M., *et al*. (2009) A microbial polysaccharide reduces the severity of rheumatoid arthritis by influencing Th17 differentiation and proinflammatory cytokines production. *J Immunol* **183:** 191–200.

Naglik, J.R., Challacombe, S.J., and Hube, B. (2003a) *Candida albicans* secreted aspartyl proteinases in virulence and pathogenesis. *Microbiol Mol Biol Rev* **67:** 400–428, table of contents.

Naglik, J.R., Rodgers, C.A., Shirlaw, P.J., Dobbie, J.L., Fernandes-Naglik, L.L., Greenspan, D., *et al*. (2003b) Differential expression of *Candida albicans* secreted aspartyl proteinase and phospholipase B genes in humans correlates with active oral and vaginal infections. *J Infect Dis* **188:** 469–479.

Nakayasu, E.S., Sobreira, T.J., Torres, R., Jr, Ganiko, L., Oliveira, P.S., Marques, A.F., and Almeida, I.C. (2012) Improved proteomic approach for the discovery of potential vaccine targets in *Trypanosoma cruzi*. *J Proteome Res* **11:** 237–246.

Naslavsky, N., Stein, R., Yanai, A., Friedlander, G., and Taraboulos, A. (1997) Characterization of detergent-insoluble complexes containing the cellular prion protein and its scrapie isoform. *J Biol Chem* **272:** 6324–6331.

Netea, M.G., and Marodi, L. (2010) Innate immune mechanisms for recognition and uptake of Candida species. *Trends Immunol* **31:** 346–353.

Newport, G., Kuo, A., Flattery, A., Gill, C., Blake, J.J., Kurtz, M.B., *et al*. (2003) Inactivation of Kex2p diminishes the virulence of *Candida albicans*. *J Biol Chem* **278:** 1713–1720.

Nicola, A.M., Frases, S., and Casadevall, A. (2009) Lipophilic dye staining of *Cryptococcus neoformans* extracellular vesicles and capsule. *Eukaryot Cell* **8:** 1373–1380.

Nimrichter, L., Rodrigues, M.L., Rodrigues, E.G., and Travassos, L.R. (2005) The multitude of targets for the immune system and drug therapy in the fungal cell wall. *Microbes Infect* **7:** 789–798. [Epub 2005 Mar].

Nisini, R., Romagnoli, G., Gomez, M.J., La Valle, R., Torosantucci, A., Mariotti, S., *et al*. (2001) Antigenic properties and processing requirements of 65-kilodalton mannoprotein, a major antigen target of anti-Candida human T-cell response, as disclosed by specific human T-cell clones. *Infect Immun* **69:** 3728–3736.

Noble, S.M., French, S., Kohn, L.A., Chen, V., and Johnson, A.D. (2010) Systematic screens of a *Candida albicans* homozygous deletion library decouple morphogenetic switching and pathogenicity. *Nat Genet* **42:** 590–598.

Nucci, M., Queiroz-Telles, F., Tobon, A.M., Restrepo, A., and Colombo, A.L. (2010) Epidemiology of opportunistic fungal infections in Latin America. *Clin Infect Dis* **51:** 561–570.

Odorizzi, G., Katzmann, D.J., Babst, M., Audhya, A., and Emr, S.D. (2003) Bro1 is an endosome-associated protein that functions in the MVB pathway in *Saccharomyces cerevisiae*. *J Cell Sci* **116:** 1893–1903.

Oliveira, D.L., Nimrichter, L., Miranda, K., Frases, S., Faull, K.F., Casadevall, A., and Rodrigues, M.L. (2009) *Cryptococcus neoformans* cryoultramicrotomy and vesicle fractionation reveals an intimate association between membrane lipids and glucuronoxylomannan. *Fungal Genet Biol* **46:** 956–963.

Oliveira, D.L., Freire-de-Lima, C.G., Nosanchuk, J.D., Casadevall, A., Rodrigues, M.L., and Nimrichter, L. (2010a) Extracellular vesicles from *Cryptococcus neoformans* modulate macrophage functions. *Infect Immun* **78:** 1601–1609.

Oliveira, D.L., Nakayasu, E.S., Joffe, L.S., Guimaraes, A.J., Sobreira, T.J., Nosanchuk, J.D., *et al*. (2010b) Characterization of yeast extracellular vesicles: evidence for the participation of different pathways of cellular traffic in vesicle biogenesis. *PLoS ONE* **5:** e11113.

O'Leary, S., O'sullivan, M.P., and Keane, J. (2011) IL-10 blocks phagosome maturation in mycobacterium tuberculosis-infected human macrophages. *Am J Respir Cell Mol Biol* **45:** 172–180.

Pappas, P.G., Rex, J.H., Sobel, J.D., Filler, S.G., Dismukes, W.E., Walsh, T.J., and Edwards, J.E. (2004) Guidelines for treatment of candidiasis. *Clin Infect Dis* **38:** 161–189.

Pfaller, M.A., and Diekema, D.J. (2007) Epidemiology of invasive candidiasis: a persistent public health problem. *Clin Microbiol Rev* **20:** 133–163.

Pietrella, D., Mazzolla, R., Lupo, P., Pitzurra, L., Gomez, M.J., Cherniak, R., and Vecchiarelli, A. (2002) Mannoprotein from *Cryptococcus neoformans* promotes T-helper type 1 anticandidal responses in mice. *Infect Immun* **70:** 6621–6627.

Pietrella, D., Bistoni, G., Corbucci, C., Perito, S., and Vecchiarelli, A. (2006) *Candida albicans* mannoprotein influences the biological function of dendritic cells. *Cell Microbiol* **8:** 602–612.

Pitarch, A., Diez-Orejas, R., Molero, G., Pardo, M., Sanchez, M., Gil, C., and Nombela, C. (2001) Analysis of the serologic response to systemic *Candida albicans* infection in a murine model. *Proteomics* **1:** 550–559.

Pitarch, A., Abian, J., Carrascal, M., Sanchez, M., Nombela, C., and Gil, C. (2004) Proteomics-based identification of novel *Candida albicans* antigens for diagnosis of systemic candidiasis in patients with underlying hematological malignancies. *Proteomics* **4:** 3084–3106.

Pitarch, A., Jimenez, A., Nombela, C., and Gil, C. (2006) Decoding serological response to Candida cell wall immunome into novel diagnostic, prognostic, and

therapeutic candidates for systemic candidiasis by proteomic and bioinformatic analyses. *Mol Cell Proteomics* **5:** 79–96.

van der Poel, S., Wolthoorn, J., van den Heuvel, D., Egmond, M., Groux-Degroote, S., Neumann, S., *et al*. (2011) Hyperacidification of trans-Golgi network and endo/lysosomes in melanocytes by glucosylceramide-dependent V-ATPase activity. *Traffic* **12:** 1634–1647.

Puccia, R., Schenkman, S., Gorin, P.A., and Travassos, L.R. (1986) Exocellular components of *Paracoccidioides brasiliensis*: identification of a specific antigen. *Infect Immun* **53:** 199–206.

Rittershaus, P.C., Kechichian, T.B., Allegood, J.C., Merrill, A.H., Jr, Hennig, M., Luberto, C., and Del Poeta, M. (2006) Glucosylceramide synthase is an essential regulator of pathogenicity of *Cryptococcus neoformans*. *J Clin Invest* **116:** 1651–1659.

Rivera, J., Cordero, R.J., Nakouzi, A.S., Frases, S., Nicola, A., and Casadevall, A. (2010) *Bacillus anthracis* produces membrane-derived vesicles containing biologically active toxins. *Proc Natl Acad Sci U S A* **107:** 19002–19007.

Rodrigues, M.L., Nimrichter, L., Oliveira, D.L., Frases, S., Miranda, K., Zaragoza, O., *et al*. (2007) Vesicular polysaccharide export in *Cryptococcus neoformans* is a eukaryotic solution to the problem of fungal trans-cell wall transport. *Eukaryot Cell* **6:** 48–59.

Rodrigues, M.L., Nakayasu, E.S., Oliveira, D.L., Nimrichter, L., Nosanchuk, J.D., Almeida, I.C., and Casadevall, A. (2008) Extracellular vesicles produced by *Cryptococcus neoformans* contain protein components associated with virulence. *Eukaryot Cell* **7:** 58–67.

Rodrigues, M.L., Franzen, A.J., Nimrichter, L., and Miranda, K. (2013) Vesicular mechanisms of traffic of fungal molecules to the extracellular space. *Curr Opin Microbiol* **16:** 414–420.

Romani, L. (2000) Innate and adaptive immunity in *Candida albicans* infections and saprophytism. *J Leukoc Biol* **68:** 175–179.

Roy, N., Barman, S., Ghosh, A., Pal, A., Chakraborty, K., Das, S.S., *et al*. (2010) Immunogenicity and protective efficacy of *Vibrio cholerae* outer membrane vesicles in rabbit model. *FEMS Immunol Med Microbiol* **60:** 18–27.

Ruchel, R., Uhlemann, K., and Boning, B. (1983) Secretion of acid proteinases by different species of the genus Candida. *Zentralbl Bakteriol Mikrobiol Hyg A* **255:** 537–548.

Sandini, S., Stringaro, A., Arancia, S., Colone, M., Mondello, F., Murtas, S., *et al*. (2011) The MP65 gene is required for cell wall integrity, adherence to epithelial cells and biofilm formation in *Candida albicans*. *BMC Microbiol* **11:** 106.

Schnaar, R.L. (1994) Isolation of glycosphingolipids. *Methods Enzymol* **230:** 348–370.

Silverman, J.M., Chan, S.K., Robinson, D.P., Dwyer, D.M., Nandan, D., Foster, L.J., and Reiner, N.E. (2008) Proteomic analysis of the secretome of *Leishmania donovani*. *Genome Biol* **9:** R35.

Silverman, J.M., Clos, J., de Oliveira, C.C., Shirvani, O., Fang, Y., Wang, C., *et al*. (2010a) An exosome-based secretion pathway is responsible for protein export from *Leishmania* and communication with macrophages. *J Cell Sci* **123:** 842–852.

Silverman, J.M., Clos, J., Horakova, E., Wang, A.Y., Wiesgigl, M., Kelly, I., *et al*. (2010b) *Leishmania* exosomes modulate innate and adaptive immune responses through effects on monocytes and dendritic cells. *J Immunol* **185:** 5011–5022.

Sorgo, A.G., Heilmann, C.J., Dekker, H.L., Brul, S., de Koster, C.G., and Klis, F.M. (2010) Mass spectrometric analysis of the secretome of *Candida albicans*. *Yeast* **27:** 661–672.

Sprong, H., Degroote, S., Claessens, T., van Drunen, J., Oorschot, V., Westerink, B.H., *et al*. (2001) Glycosphingolipids are required for sorting melanosomal proteins in the Golgi complex. *J Cell Biol* **155:** 369–380.

Stanley, E.R., and Heard, P.M. (1977) Factors regulating macrophage production and growth. Purification and some properties of the colony stimulating factor from medium conditioned by mouse L cells. *J Biol Chem* **252:** 4305–4312.

Thomas, D.P., Lopez-Ribot, J.L., and Lee, S.A. (2009) A proteomic analysis of secretory proteins of a pre-vacuolar mutant of *Candida albicans*. *J Proteomics* **73:** 342–351.

Tian, T., Wang, Y., Wang, H., Zhu, Z., and Xiao, Z. (2010) Visualizing of the cellular uptake and intracellular trafficking of exosomes by live-cell microscopy. *J Cell Biochem* **111:** 488–496.

Torosantucci, A., Gomez, M.J., Bromuro, C., Casalinuovo, I., and Cassone, A. (1991) Biochemical and antigenic characterization of mannoprotein constituents released from yeast and mycelial forms of *Candida albicans*. *J Med Vet Mycol* **29:** 361–372.

Trocoli Torrecilhas, A.C., Tonelli, R.R., Pavanelli, W.R., da Silva, J.S., Schumacher, R.I., de Souza, W., *et al*. (2009) *Trypanosoma cruzi*: parasite shed vesicles increase heart parasitism and generate an intense inflammatory response. *Microbes Infect* **11:** 29–39.

Vallejo, M.C., Matsuo, A.L., Ganiko, L., Medeiros, L.C., Miranda, K., Silva, L.S., *et al*. (2011) The pathogenic fungus *Paracoccidioides brasiliensis* exports extracellular vesicles containing highly immunogenic alpha-Galactosyl epitopes. *Eukaryot Cell* **10:** 343–351.

Vallejo, M.C., Nakayasu, E.S., Longo, L.V., Ganiko, L., Lopes, F.G., Matsuo, A.L., *et al*. (2012a) Lipidomic analysis of extracellular vesicles from the pathogenic phase of *Paracoccidioides brasiliensis*. *PLoS ONE* **7:** e39463.

Vallejo, M.C., Nakayasu, E.S., Matsuo, A.L., Sobreira, T.J., Longo, L.V., Ganiko, L., *et al*. (2012b) Vesicle and vesicle-free extracellular proteome of *Paracoccidioides brasiliensis*: comparative analysis with other pathogenic fungi. *J Proteome Res* **11:** 1676–1685.

van de Veerdonk, F.L., Kullberg, B.J., and Netea, M.G. (2012) Adjunctive immunotherapy with recombinant cytokines for the treatment of disseminated candidiasis. *Clin Microbiol Infect* **18:** 112–119.

Vyas, K.A., Patel, H.V., Vyas, A.A., and Schnaar, R.L. (2001) Segregation of gangliosides GM1 and GD3 on cell membranes, isolated membrane rafts, and defined supported lipid monolayers. *Biol Chem* **382:** 241–250.

Youseff, B.H., Holbrook, E.D., Smolnycki, K.A., and Rappleye, C.A. (2012) Extracellular superoxide dismutase

protects Histoplasma yeast cells from host-derived oxidative stress. *PLoS Pathog* **8:** e1002713.

Supporting information

Additional Supporting Information may be found in the online version of this article at the publisher's web-site:

Table S1. Protein groups and individual proteins identified from *Candida albicans* (strains 11 and ATCC 90028) EV by proteomic analysis. (Note: please see row color codes at the bottom of the table).

Table S2. Biological and molecular functions of *Candida albicans* EV proteins identified by proteomic analysis.